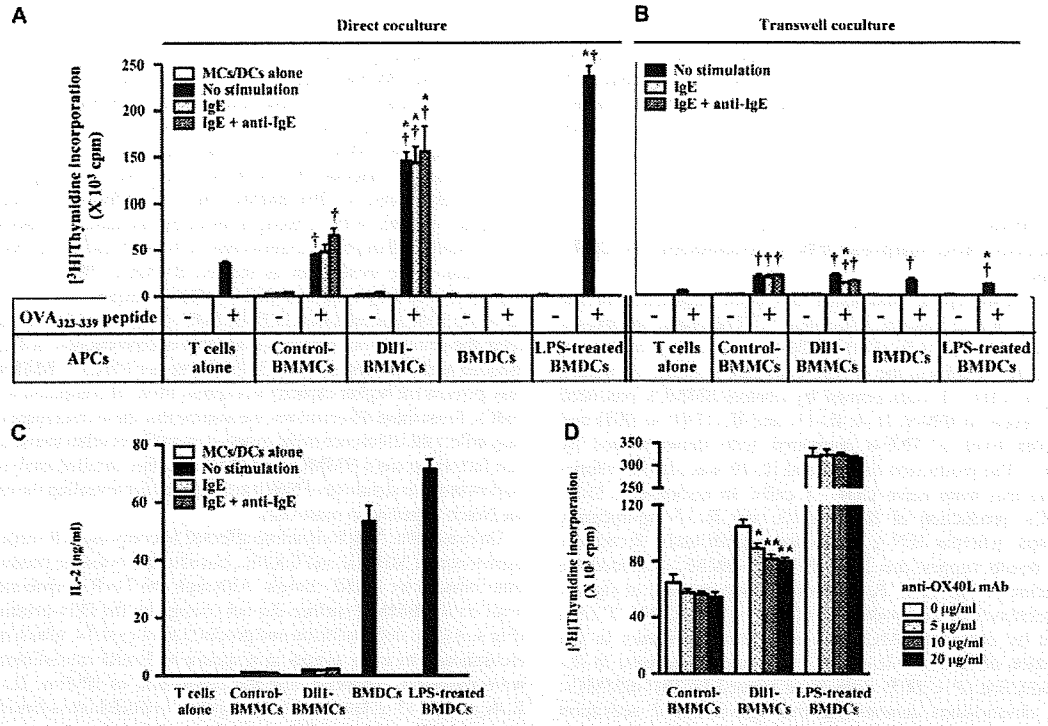

FIG 5. $CD4^+$ T-cell activation mediated by Dll1-BMMCs. [^{3}H]Thymidine incorporation into the $CD4^+$ T cells from DO11.10 mice cocultured together with BMMCs or BMDCs (A) or separated from them by a Transwell membrane (B) in the presence or absence of ovalbumin (*OVA*) peptide. Data are indicated as means ± SDs of triplicate samples. †$P < .05$ vs T cells alone in the presence of OVA peptide; *$P < .05$ vs corresponding values for T cells plus control-BMMCs. *MC*, Mast cell; *DC*, dendritic cell. C, IL-2 level in the supernatants when $CD4^+$ T cells from DO11.10 mice were direct cocultured with BMMCs or BMDCs at 48 hours in the presence of OVA peptide. Data are indicated as means ± SDs of triplicate samples. D, [^{3}H]Thymidine incorporation into the $CD4^+$ T cells from DO11.10 mice direct cocultured with BMMCs or BMDCs in the presence of OVA peptide and anti-OX40L neutralizing mAb at indicated concentrations. Data are indicated as means ± SDs of triplicate samples. *$P < .05$; **$P < .005$, significantly different as determined by the Student *t* test compared with the corresponding control.

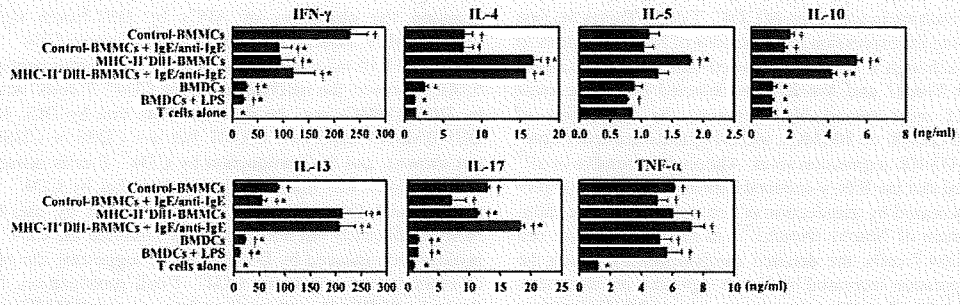

FIG 6. Dll1-BMMCs enhance IL-4, IL-10, and IL-13 production and suppress IFN-γ production by $CD4^+$ T cells. Purified $CD4^+$ T cells from DO11.10 mice were direct cocultured with BMMCs or BMDCs in the presence of ovalbumin peptide. After 4 days of coculture, the cocultured cells were restimulated with anti-CD3 mAb and anti-CD28 mAb for 24 hours, and then the cytokine concentrations in the supernatants were measured. Data are indicated as means ± SDs of triplicate samples. †$P < .05$ vs T cells alone; *$P < .05$ vs T cells plus control-BMMCs.

contrast, the direct interaction with MHC-II$^+$ Dll1-BMMCs promoted $CD4^+$ T cells to produce the T_H2 cytokines IL-4, IL-5, IL-10, and IL-13. The $CD4^+$ T cells primed by MHC-II$^+$ Dll1-BMMCs seem to have the characteristics of conventional T_H2 cells.[42] It has been reported that keratinocytes, dendritic cells, bone marrow stroma, and thymic epithelium express Notch ligands including Dll1.[43,44] Therefore, tissue-resident mast cells may be primed by Notch ligands expressed in their microenvironment. Mast cells then migrate to the spleen and lymph nodes under inflammatory conditions and influence the development and character of the immune response.[14,15] The proximity of mast cells and T cells in these organs allows mast cells to influence the priming of

naive T cells directly. Regardless, further *in vivo* analysis is required to clarify the roles of mast cells primed by Notch ligands.

Our findings in the current study suggest that Dll1/Notch signaling induces the commitment of mast cells to an APC population, which induce the differentiation of naive $CD4^+$ T cells toward conventional T_H2 cells. Further studies on the role of mast cells in the sensitization phase of acquired immune responses will contribute to the prevention and/or treatment of infectious diseases, autoimmune disorders, and allergic disorders.

We thank the members of Atopy (Allergy) Research Center and the Department of Immunology of the Juntendo University School of Medicine for their comments, encouragement, and technical assistance, and we thank Ms Michiyo Matsumoto for secretarial assistance.

Clinical implications: The findings that mast cells acquire APC functions by Notch signaling and induce the differentiation of T_H2 will contribute to the elucidation of the pathogenic mechanism of allergic disorders.

REFERENCES

1. Supajatura V, Ushio H, Nakao A, Okumura K, Ra C, Ogawa H. Protective roles of mast cells against enterobacterial infection are mediated by Toll-like receptor 4. J Immunol 2001;167:2250-6.
2. Marshall JS, Jawdat DM. Mast cells in innate immunity. J Allergy Clin Immunol 2004;114:21-7.
3. Nakano N, Nishiyama C, Kunada S, Niwa Y, Shimokawa N, Ushio H, et al. Involvement of mast cells in IL-12/23 p40 production is essential for survival from polymicrobial infections. Blood 2007;109:4846-55.
4. Metz M, Grimbaldeston MA, Nakae S, Piliponsky AM, Tsai M, Galli SJ. Mast cells in the promotion and limitation of chronic inflammation. Immunol Rev 2007;217:304-28.
5. Sayed BA, Brown MA. Mast cells as modulators of T-cell responses. Immunol Rev 2007;217:53-64.
6. Biedermann T, Kneilling M, Mailhammer R, Maier K, Sander CA, Kollias G, et al. Mast cells control neutrophil recruitment during T cell-mediated delayed-type hypersensitivity reactions through tumor necrosis factor and macrophage inflammatory protein 2. J Exp Med 2000;192:1441-52.
7. Williams CM, Galli SJ. Mast cells can amplify airway reactivity and features of chronic inflammation in an asthma model in mice. J Exp Med 2000;192:455-62.
8. Lee DM, Friend DS, Gurish MF, Benoist C, Mathis D, Brenner MB. Mast cells: a cellular link between autoantibodies and inflammatory arthritis. Science 2002;297:1689-92.
9. Araki Y, Andoh A, Fujiyama Y, Bamba T. Development of dextran sulphate sodium-induced experimental colitis is suppressed in genetically mast cell-deficient Ws/Ws rats. Clin Exp Immunol 2000;119:264-9.
10. Secor VH, Secor WE, Gutekunst CA, Brown MA. Mast cells are essential for early onset and severe disease in a murine model of multiple sclerosis. J Exp Med 2000;191:813-22.
11. Robbie-Ryan M, Brown M. The role of mast cells in allergy and autoimmunity. Curr Opin Immunol 2002;14:728-33.
12. Galli SJ, Nakae S, Tsai M. Mast cells in the development of adaptive immune responses. Nat Immunol 2005;6:135-42.
13. Nakae S, Suto H, Berry GJ, Galli SJ. Mast cell-derived TNF can promote Th17 cell-dependent neutrophil recruitment in ovalbumin-challenged OTII mice. Blood 2007;109:3640-8.
14. Wang HW, Tedla N, Lloyd AR, Wakefield D, McNeil PH. Mast cell activation and migration to lymph nodes during induction of an immune response in mice. J Clin Invest 1998;102:1617-26.
15. Tanzola MB, Robbie-Ryan M, Gutekunst CA, Brown MA. Mast cells exert effects outside the central nervous system to influence experimental allergic encephalomyelitis disease course. J Immunol 2003;171:4385-91.
16. Kashiwakura J, Yokoi H, Saito H, Okayama Y. T cell proliferation by direct cross-talk between OX40 ligand on human mast cells and OX40 on human T cells: comparison of gene expression profiles between human tonsillar and lung-cultured mast cells. J Immunol 2004;173:5247-57.
17. Nakae S, Suto H, Iikura M, Kakurai M, Sedgwick JD, Tsai M, et al. Mast cells enhance T cell activation: importance of mast cell costimulatory molecules and secreted TNF. J Immunol 2006;176:2238-48.
18. Kambayashi T, Baranski JD, Baker RG, Zou T, Allenspach EJ, Shoag JE, et al. Indirect involvement of allergen-captured mast cells in antigen presentation. Blood 2007;111:1489-96.
19. Raposo G, Tenza D, Mecheri S, Peronet R, Bonnerot C, Desaymard C. Accumulation of major histocompatibility complex class II molecules in mast cell secretory granules and their release upon degranulation. Mol Biol Cell 1997;8:2631-45.
20. Koch N, Wong GH, Schrader JW. Ia antigens and associated invariant chain are induced simultaneously in lines of T-dependent mast cells by recombinant interferon-gamma. J Immunol 1984;132:1361-9.
21. Frandji P, Oskeritzian C, Cacaraci F, Lapeyre J, Peronet R, David B, et al. Antigen-dependent stimulation by bone marrow-derived mast cells of MHC class II-restricted T cell hybridoma. J Immunol 1993;151:6318-28.
22. Fox CC, Jewell SD, Whitacre CC. Rat peritoneal mast cells present antigen to a PPD-specific T cell line. Cell Immunol 1994;158:253-64.
23. Nishiyama C, Nishiyama M, Ito T, Masuki S, Maeda K, Masuoka N, et al. Overproduction of PU.1 in mast cell progenitors: its effect on monocyte- and mast cell-specific gene expression. Biochem Biophys Res Commun 2004;313:516-21.
24. Ito T, Nishiyama C, Nishiyama M, Matsuda H, Maeda K, Akizawa Y, et al. Mast cells acquire monocyte-specific gene expression and monocyte-like morphology by overproduction of PU.1. J Immunol 2005;174:376-83.
25. Schroeder T, Kohlhof H, Rieber N, Just U. Notch signaling induces multilineage myeloid differentiation and up-regulates PU.1 expression. J Immunol 2003;170:5538-48.
26. Geffers I, Serth K, Chapman G, Jaekel R, Schuster-Gossler K, Cordes R, et al. Divergent functions and distinct localization of the Notch ligands DLL1 and DLL3 in vivo. J Cell Biol 2007;178:465-76.
27. Luo D, Renault VM, Rando TA. The regulation of Notch signaling in muscle stem cell activation and postnatal myogenesis. Semin Cell Dev Biol 2005;16:612-22.
28. Louvi A, Artavanis-Tsakonas S. Notch signalling in vertebrate neural development. Nat Rev Neurosci 2006;7:93-102.
29. Gaiano N, Fishell G. The role of notch in promoting glial and neural stem cell fates. Annu Rev Neurosci 2002;25:471-90.
30. Taniguki K, Honjo T. Regulation of lymphocyte development by Notch signaling. Nat Immunol 2007;8:451-6.
31. Osborne BA, Minter LM. Notch signalling during peripheral T-cell activation and differentiation. Nat Rev Immunol 2007;7:64-75.
32. Jönsson JI, Xiang Z, Pettersson M, Lardelli M, Nilsson G. Distinct and regulated expression of Notch receptors in hematopoietic lineages and during myeloid differentiation. Eur J Immunol 2001;31:3240-7.
33. Murphy KM, Heimberger AB, Loh DY. Induction by antigen of intrathymic apoptosis of CD4+CD8+TCRlo thymocytes in vivo. Science 1990;250:1720-3.
34. Shimizu K, Chiba S, Hosoya N, Kumano K, Saito T, Kurokawa M, et al. Binding of Delta1, Jagged1, and Jagged2 to Notch2 rapidly induces cleavage, nuclear translocation, and hyperphosphorylation of Notch2. Mol Cell Biol 2000;20:6913-22.
35. Moriyama Y, Sekine C, Koyanagi A, Koyama N, Ogata H, Chiba S, et al. Delta-like 1 is essential for the maintenance of marginal zone B cells in normal mice but not in autoimmune mice. Int Immunol 2008;20:763-73.
36. Hadland BK, Manley NR, Su D, Longmore GD, Moore CL, Wolfe MS, et al. Gamma-secretase inhibitors repress thymocyte development. Proc Natl Acad Sci U S A 2001;98:7487-91.
37. Doerfler P, Shearman MS, Perlmutter RM. Presenilin-dependent gamma-secretase activity modulates thymocyte development. Proc Natl Acad Sci U S A 2001;98:9312-7.
38. Ohshima Y, Yang LP, Uchiyama T, Tanaka Y, Baum P, Sergerie M, et al. OX40 costimulation enhances interleukin-4 (IL-4) expression at priming and promotes the differentiation of naive human CD4(+) T cells into high IL-4-producing effectors. Blood 1998;92:3338-45.
39. Akiba H, Miyahira Y, Atsuta M, Takeda K, Nohara C, Futagawa T, et al. Critical contribution of OX40 ligand to T helper cell type 2 differentiation in experimental leishmaniasis. J Exp Med 2000;191:375-80.
40. Monsalve E, Perez MA, Rubio A, Ruiz-Hidalgo MJ, Baladron V, Garcia-Ramirez JJ, et al. Notch-1 up-regulation and signaling following macrophage activation modulates gene expression patterns known to affect antigen-presenting capacity and cytotoxic activity. J Immunol 2006;176:5362-73.
41. Rekhtman N, Radparvar F, Evans T, Skoultchi AI. Direct interaction of hematopoietic transcription factors PU.1 and GATA-1: functional antagonism in erythroid cells. Genes Dev 1999;13:1398-411.
42. O'Garra A. Cytokines induce the development of functionally heterogeneous T helper cell subsets. Immunity 1998;8:275-83.
43. Thelu J, Rossio P, Favier B. Notch signalling is linked to epidermal cell differentiation level in basal cell carcinoma, psoriasis and wound healing. BMC Dermatol 2002;2:7.
44. Maillard I, Adler SH, Pear WS. Notch and the immune system. Immunity 2003;19:781-91.

Tim-3 mediates phagocytosis of apoptotic cells and cross-presentation

Masafumi Nakayama,[1] Hisaya Akiba,[1] Kazuyoshi Takeda,[1] Yuko Kojima,[2] Masaaki Hashiguchi,[3] Miyuki Azuma,[3] Hideo Yagita,[1] and Ko Okumura[1]

[1]Department of Immunology and [2]Division of Biomedical Imaging Research, Biomedical Research Center, Juntendo University School of Medicine, Tokyo; and [3]Department of Molecular Immunology, Graduate School, Tokyo Medical and Dental University, Tokyo, Japan

Phagocytes such as macrophages and dendritic cells (DCs) engulf apoptotic cells to maintain peripheral immune tolerance. However, the mechanism for the recognition of dying cells by phagocytes is not fully understood. Here, we demonstrate that T-cell immunoglobulin mucin-3 (Tim-3) recognizes apoptotic cells through the FG loop in the IgV domain, and is crucial for clearance of apoptotic cells by phagocytes. Whereas Tim-4 is highly expressed on peritoneal resident macrophages, Tim-3 is expressed on peritoneal exudate macrophages, monocytes, and splenic DCs, indicating distinct Tim-mediated phagocytic pathways used by different phagocytes. Furthermore, phagocytosis of apoptotic cells by CD8$^+$ DCs is inhibited by anti–Tim-3 mAb, resulting in a reduced cross-presentation of dying cell-associated antigens in vitro and in vivo. Administration of anti–Tim-3 as well as anti–Tim-4 mAb induces autoantibody production. These results indicate a crucial role for Tim-3 in phagocytosis of apoptotic cells and cross-presentation, which may be linked to peripheral tolerance. (Blood. 2009;113: 3821-3830)

Introduction

Apoptosis is a crucial process in the development and homeostasis of multicellular organisms.[1,2] In the immune system, an enormous number of cells undergo apoptosis during development of lymphocytes and after interaction with antigens.[3] Because apoptotic cells and secondary necrotic cells releasing intracellular contents could be autoantigens, phagocytes such as macrophages and dendritic cells (DCs) must engulf these dying cells rapidly and efficiently to prevent detrimental inflammatory responses and autoimmunity.[1,4] To engulf apoptotic cells, macrophages use a variety of molecules, including Mer tyrosine kinase (MerTK),[5] milk fat globule-EGF-factor 8 (MFG-E8),[6] brain-specific angiogenesis inhibitor 1 (BAI1),[7] and T-cell immunoglobulin and mucin domain-containing molecule 4 (Tim-4).[8,9] However, their relative contributions to the phagocytosis remain to be elucidated. Multiple receptors may simultaneously recognize multiple "eat-me" signals on apoptotic cells. In addition, different subsets of macrophages may use different repertoires of receptors for the phagocytosis.

DCs are able to not only phagocytose apoptotic cells but also present dying cell-associated antigens with MHC class I molecules, which is termed as "cross-presentation."[1,10] It has been considered that, in steady state, cross-presentation of self-antigens by DCs stimulates CD8$^+$ T cells to proliferate abortively, resulting in their deletion, which is crucial to maintain peripheral tolerance.[10-14] Among mouse splenic DC subsets, CD8$^+$ DCs are unique in their ability for efficient phagocytosis of apoptotic cells and cross-presentation.[15,16] However, the mechanism for the recognition of apoptotic cells by CD8$^+$ DCs is poorly understood. Scavenger receptor CD36 and mannose receptor (MR)/DEC205 are highly expressed on CD8$^+$ DCs, but not CD8$^-$ DCs, however, these receptors are not required for cross-presentation of cell-associated antigens by this DC subset.[16-18] Neither $\alpha_v\beta_3$ nor $\alpha_v\beta_5$ integrin that mediates phagocytosis of apoptotic cells by macrophages[1] is essential for phagocytosis by CD8$^+$ DCs.[17] Thus, the phagocytic receptor for apoptotic cells linked to cross-presentation remains to be identified.

Tim-3 has been identified as a Th1-specific marker, and several in vivo studies have shown that Tim-3 regulates autoimmunity.[19,20] We and others have reported that Tim-3 negatively regulates Th1-mediated inflammatory diseases such as experimental autoimmune encephalomyelitis (EAE), type I diabetes, and acute graft-versus-host diseases (aGVHD).[21-23] Moreover, it has been reported that Tim-3 promotes tolerance induction.[21,22] Recently, Zhu et al have identified galectin-9 as a Tim-3 ligand, and they have demonstrated that galectin-9 binds to the carbohydrate chains on Tim-3, and induces cell death of Th1 cells in vitro, which may explain the mechanism by which Tim-3 suppresses Th1 immunity.[24] On the other hand, Anderson et al have reported that Tim-3 is expressed on DCs, and that galectin-9 activates the DCs through Tim-3, proposing that Tim-3 exacerbates EAE.[25] Taken together, Tim-3 appears to have multiple roles for the immune regulation in vivo, however, it remains unknown whether these multiple functions of Tim-3 are mediated solely through galectin-9.

In this study, we demonstrate that Tim-3 recognizes apoptotic cells through the FG loop in the IgV domain. Although Tim-4 is reported to be crucial for the phagocytosis of apoptotic cells by peritoneal macrophages,[8,9] we highlight here Tim-3 as the phagocytic receptor responsible for cross-presentation of dying cell-associated antigens by CD8$^+$ DCs. We propose that this novel function of Tim-3 may be involved in autoimmune regulation and tolerance induction.

Submitted October 23, 2008; accepted February 5, 2009. Prepublished online as *Blood* First Edition paper, February 17, 2009; DOI 10.1182/blood-2008-10-185884.

The online version of this article contains a data supplement.

The publication costs of this article were defrayed in part by page charge payment. Therefore, and solely to indicate this fact, this article is hereby marked "advertisement" in accordance with 18 USC section 1734.

Methods

Mice and reagents

Five-week-old female C57BL/6 mice were obtained from Charles River Japan (Yokohama, Japan). OT-I mice expressing $OVA_{257-264}$/H-$2K^b$–specific TCR were kindly provided by W. R. Heath (The Walter and Eliza Hall Institute, Melbourne, Australia) through H. Udono (RCAI, RIKEN, Yokohama, Japan). These mice were maintained under specific pathogen-free conditions, and used according to the guidelines of the institutional animal care and use committee established at Juntendo University and Tokyo Medical and Dental University. pcDNA3.1(−), pEF6/V5-TOPO, and pcDNA3.1-GFP-TOPO vectors were purchased from Invitrogen (Frederick, MD). PE-Mac1 (CD11b) mAb and control rat IgG2a were purchased from eBioscience (San Diego, CA). FITC-anti-CD11c mAb, PE-anti-Vα2 mAb, and allophycocyanin (APC)–anti-CD8α mAb were purchased from BD Biosciences (San Jose, CA). Alexa Fluor 647–anti-CD8α mAb was purchased from Biolegend (San Diego, CA). 5-(and-6)-Carboxyfluorescein diacetate succinimidyl ester (CFSE) and 5-(and-6)-carboxytetramethylrhodamine succinimidyl ester (TAMRA) were purchased from Invitrogen. TdT and biotin-16-dUTP were purchased from Roche (Indianapolis, IN).

Generation of Tim-Igs and mAbs

The expression vectors for Tim-1–Ig, Tim-2–Ig, Tim-3–Ig, and Tim-4–Ig were generated by linking the extracellular domains of Tim-1 (aa 1-236), Tim-2 (aa 1-230), Tim-3 (aa 1-191), or Tim-4 (aa 1-288) to the Fc portion of mouse IgG2a in the pcDNA3.1(−) vector. Tim-Ig proteins were produced by transfection of each vector into HEK293T cells. The anti–mouse Tim-1 mAb (RMT1-17, rat IgG2a, κ), Tim-2 mAb (RMT2-14, rat IgG2a, κ), and Tim-3 mAb (RMT3-23, rat IgG2a, κ) were generated immunizing SD rats with Tim-1–Ig, Tim-2–Ig, and Tim-3–Ig, respectively, as described before.[23] Likewise, the anti–Tim-4 mAb (RMT4-54, rat IgG2a, κ) was generated by immunizing an SD rat with Tim-4–Ig, fusing lymph node cells with P3U1 myeloma cells, and screening the binding to CHO cells expressing Tim-4, but not parental CHO cells. For confocal microscopy, RMT3-23 was labeled with Alexa Fluor 594 using the mAb labeling kit (Invitrogen). Requests for mAbs should be addressed to H. Akiba (e-mail: hisaya@juntendo.ac.jp).

Cell lines

A normal rat kidney cell line (NRK-52E) was maintained in complete RPMI medium (RPMI 1640 supplemented with 10% FBS, 100 U/mL penicillin, 100 μg/mL streptomycin, and 2 mM glutamine, 10 mM HEPES, and 50 μM 2-mercaptoethanol). HEK293T cells (ATCC, Manassas, VA) were maintained in complete DMEM medium (DMEM supplemented with 10% FBS, 100 U/mL penicillin, 100 μg/mL streptomycin, and 2 mM glutamine). For construction of expression vectors, the entire coding region of mouse Tim-1, Tim-2, Tim-3, or Tim-4 was subcloned into pMKITneo. Tim-3 cDNA was also subcloned into pEF6/V5-TOPO vector. Several mutant forms were prepared by polymerase chain reaction (PCR)–based mutagenesis using Tim-3/pEF6V5-TOPO as a template. After confirmation of nucleotide sequences, Tim expression vectors were transduced into NRK cells by electroporation with a Gene Pulser (Bio-Rad Laboratories, Hercules, CA). After selection with 1 mg/mL G418, cell surface expression was estimated by respective anti-Tim mAbs. HEK293T cells were transiently transfected with these expression vectors using lipofectAMINE2000 (Invitrogen). Two days after the transfection, cell surface expression of Tim was estimated by flow cytometry.

Phagocytosis assay

For preparation of apoptotic cells, thymocytes from C57BL/6 mice were labeled with 1 μM CFSE or 10 μg/mL TAMRA, and then were UV irradiated (100 J/cm^2). After UV irradiation, the cells were cultured in complete RPMI for 2 hours at 37°C, and then used for the phagocytosis assay. NRK cells (10^5 per well), NIH3T3 cells (5×10^4 cells per well), and HEK293T cells (10^5 cells per well) were plated onto 24-well plates, which were precoated with poly-L-lysine for HEK293T cells, a day before the phagocytosis assay. These cell lines were incubated with fluorescently labeled apoptotic cells (2×10^6 per well) at 37°C for the indicated periods. The recognition (binding and/or incorporation) of fluorescently labeled apoptotic cells by these cell lines was analyzed by flow cytometry using a FACSCalibur (BD Biosciences) and/or fluorescence microscopy using an Olympus FV1000 laser scanning confocal microscope (Melville, NY) equipped with 40× or 100× objective lens. For macrophages, peritoneal cells were harvested from C57BL/6 mice 3 days after intraperitoneal injection of 2 mL 3% wt/vol thioglycolate, or from untreated mice. These peritoneal cells (5×10^5 per well) were plated onto 48-well plate for 2 hours at 37°C, and then washed with PBS twice to remove floating cells. In some assay, macrophages were preincubated with the indicated mAb (30 μg/mL) for 60 minutes at 4°C, and then washed with PBS to remove unbound mAb. Macrophages were cultured with fluorescently labeled apoptotic cells (2.5×10^6 per well) for 30 minutes at 37°C, and then washed with PBS 3 times to remove unbound apoptotic cells. After trypsinization, cells were harvested and stained with PE-Mac1. CFSE fluorescence intensity in Mac1$^+$ cells was analyzed on a FACSCalibur (BD Biosciences). As for an in vivo phagocytosis by PEM, sterile peritonitis was induced in C57BL/6 mice by intraperitoneal injection of 3% thioglycolate medium (2 mL per mouse). Three days later, these mice (n = 4-5 per group) were treated intraperitoneally with control rat IgG (rIgG), RMT3-23, or RMT4-54 (200 μg/mouse). Three hours later, mice were intraperitoneally injected with CFSE-labeled apoptotic cells (10^8 per mouse), and another 2 hours later, peritoneal cells were harvested. The recognition of apoptotic cells by Mac1$^+$ cells was analyzed by flow cytometry. For statistic evaluation, the unpaired Student *t* test, 2-tailed was used. *P* values less than .05 were considered significant. For in vitro phagocytosis assay using splenic DCs, spleens were digested with 400 U/mL collagenase (Wako Biochemicals) in the presence of 5 mM EDTA and separated into low- and high-density fractions on Optiprep gradient (Axis-Shield, Oslo, Norway). Low-density cells were purified using anti-CD11c MACS beads (Miltenyi Biotec, Auburn, CA). After staining CD11c$^+$ cells with APC-anti-CD8α mAb, these cells (5×10^5 per well) were cocultured with TAMRA-labeled apoptotic cells (2.5×10^6 per well) in 48-well plate for the indicated periods, and then the cells were stained with FITC–anti-CD11c mAb. TAMRA fluorescence intensity in CD8$^-$CD11c$^+$ and CD8$^+$CD11c$^+$ cells was analyzed on a FACSCalibur. As for in vivo phagocytosis by splenic DCs, mice (n = 3 per group) were treated intravenously with rIgG, or RMT3-23 and/or RMT4-54 (200 μg each/mouse), and then 2 hours later, with CFSE-labeled apoptotic splenocytes (2×10^7 per mouse). Mice were killed at the indicated time points, and the recognition of apoptotic cells by CD8$^+$CD11c$^+$ cells was analyzed by flow cytometry. For statistic evaluation, the unpaired Student *t* test, 2-tailed was used. *P* values less than .05 were considered significant.

In situ identification of nuclear DNA fragmentation

C57BL/mice (n = 4-6 per group) were treated intraperitoneally with rIgG, or RMT3-23 and/or RMT4-54 (200 μg each per mouse) twice a week for 4 weeks. Three days after the final injection, mice were killed. Serum was stocked for measurement of anti-dsDNA antibody levels. Brain, liver, spleen, and pancreas were immersion-fixed in 20% buffered formalin and embedded in paraffin. After being deparaffinized, tissue sections were stained using in situ TUNEL method with biotin-16-dUTP (Roche Diagnostics, Basel, Switzerland) and diaminobenzidine as a peroxidase substrate. Nuclei were counterstained with hematoxylin. The number of TUNEL-positive cells was quantified with KS400 Image Analysis System (KS400; Zeiss, Heidelberg, Germany).

Measurement of anti-dsDNA antibody levels in serum

Serum levels of anti-dsDNA IgG were determined as described previously.[26] In brief, enzyme-linked immunosorbent assay (ELISA) plates were coated with 5 μg/mL dsDNA derived from calf thymus (Sigma-Aldrich, St Louis, MO). Anti-dsDNA antibody level was expressed in units, referring to

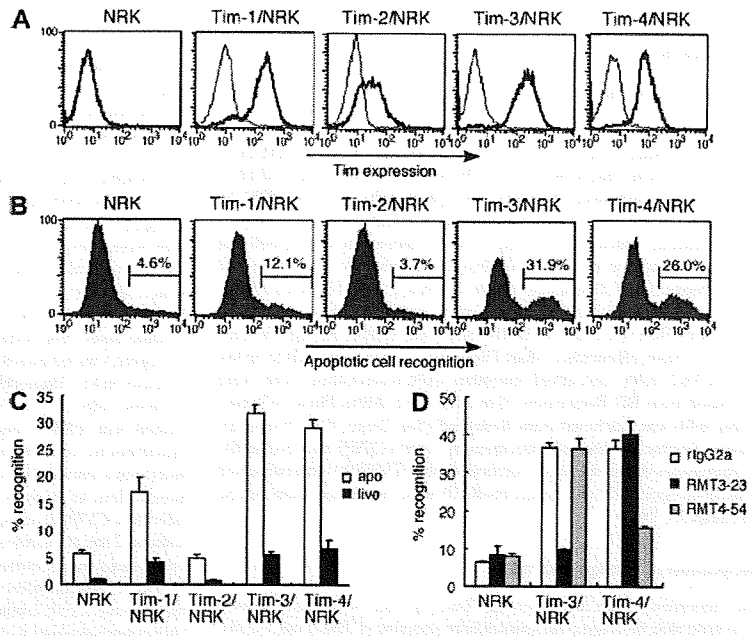

Figure 1. Tim-3 recognizes apoptotic cells. (A) NRK cells stably expressing Tim-1, Tim-2, Tim-3, or Tim-4 were stained with biotinylated anti–Tim-1 mAb (RMT1-17), anti–Tim-2 mAb (RMT2-14), anti–Tim-3 mAb (RMT3-23), or anti–Tim-4 mAb (RMT4-54), respectively. Parental NRK cells were stained with a cocktail of all mAbs. Then cells were stained with PE-avidin, and analyzed by flow cytometry (thick histogram). Thin histograms indicate background staining with control rat IgG2a, followed by PE-avidin. (B) These NRK cells were cultured with CFSE-labeled apoptotic cells for 30 minutes at 37°C. Recognition of apoptotic cells by these NRK cells was quantified by flow cytometry. (C) These NRK cells were cultured with CFSE-labeled viable cells or apoptotic cells for 30 minutes at 37°C. Percentage of the recognition was quantified by flow cytometry. Data are represented as mean ± SD of triplicates. (D) These NRK cells were pretreated with 20 μg/mL control rIgG2a, RMT3-23, or RMT4-54 mAb, and then cultured with CFSE-labeled apoptotic cells for 30 minutes at 37°C. Percentage of the recognition was quantified by flow cytometry. Data are represented as mean ± SD of triplicates. Similar results were obtained in 3 (A-C) or 2 (D) independent experiments.

standard curve obtained by serial dilution of a standard serum pool from (NZB × NZW) F1 mice older than 8 months, containing 1000 U activities/mL (kindly provided by S. Hirose, Juntendo University).

Flow cytometric analysis for Tim expression

Mouse macrophages or low-density splenocytes were pretreated with anti-FcR mAb (2.4G2), and then were incubated with 0.5 μg biotinylated mAb for 30 minutes at 4°C, followed by PE-streptavidin and FITC-anti-CD11b mAb (for macrophages) or PE-streptavidin, FITC–anti-CD11c mAb and APC–anti-CD8α mAb (for splenic DCs). After washing with PBS, Tim expression on $CD11b^+$, $CD8^+CD11c^+$, or $CD8^-CD11c^+$ cells was analyzed on a FACSCalibur, and the data were analyzed using the CellQuest program (BD Biosciences).

In vitro cross-presentation assay

OVA-loaded dying cells were prepared by osmotic shock as described previously.[12] For splenic DC subsets, $CD11c^+$ cells purified using anti-CD11c MACS beads (> 92% $CD11c^+$) were then stained with FITC–anti-CD11c and APC–anti-CD8α mAbs, followed by sorting into subsets (> 89% $CD8^+CD11c^+$; > 98% $CD8^-CD11c^+$) on FACSVantage (BD Biosciences). OVA-loaded (10 mg/mL) dying cells (2.5×10^6 per well) were cocultured with $CD8^+$ DCs or $CD8^-$ DCs (5×10^5 per well) in presence of rIgG, RMT3-23, or RMT4-54 (30 μg/mL) on 48-well plate for 1.5 hours, and then DCs were sorted again using anti-CD11c MACS beads. $CD8^-$ or $CD8^+$ DCs (both 10^4 or 2×10^3 per well) were cocultured with purified OT-I $CD8^+$ T cells (10^5 per well) in 96-well flat-bottom plate. For the direct presentation, $CD8^-$ or $CD8^+$ DCs (10^4 per well) were cocultured with 1 nM $OVA_{257-264}$ SIINFEKL peptides (AnaSpec, San Jose, CA) and OT-I $CD8^+$ T cells (10^5 per well) in presence of rIgG, RMT3-23, or RMT4-54 (30 μg/mL) in 96-well flat-bottom plate. Two days later, 50 μL supernatant was harvested and tested for IFN-γ production by sandwich ELISA (eBioscience). The cultures were then pulsed overnight with [^{3}H]thymidine (0.5 μCi [0.0185 MBq]/well; GE Healthcare, Little Chalfont, United Kingdom) and the uptake was measured in a microbeta counter (Microbeta Plus; Wallac, Turku, Finland).

In vivo cross-presentation assay

In vivo cross-presentation assay was performed as described previously[27] with minor modifications. CFSE-labeled OT-I cells (2×10^6 per mouse) were transferred intravenously into B6 mice. Next day, mice were injected intravenously with rIgG, or RMT3-23 and/or RMT4-54 (200 μg each per mouse), and then 2 hours later, with OVA-loaded (1 mg/mL) dying splenocytes (10^7 per mouse). Two days later, mice were killed, and splenocytes were stained with PE–anti-Vα2 and APC–anti-CD8. CFSE fluorescence intensity of $CD8^+V\alpha2^+$ cells was analyzed by flow cytometry.

Results

Tim-3 recognizes apoptotic cells and is recruited to phagosome

Because Tim-4 and Tim-1 are recently reported to recognize apoptotic cells,[8,9] we first verified the binding activity of NRK cells stably expressing Tim family molecules (Figure 1A) to apoptotic cells. As for apoptotic cells, we used UV (100 J/cm^2)–irradiated thymocytes because these cells show typical apoptotic phenotypes, which are annexin V^+ and propidium iodide negative (PI^-) (Figure S1A, available on the *Blood* website; see the Supplemental Materials link at the top of the online article), and do not express Tim molecules (Figure S1B), excluding Tim-Tim interaction in this study. In addition to Tim-4/NRK and Tim-1/NRK, we found that Tim-3/NRK also efficiently bound apoptotic cells, but not live cells (Figure 1B,C), and that the binding of Tim-3/NRK and Tim-4/NRK cells to apoptotic cells was abrogated by anti–Tim-3 mAb RMT3-23 and anti–Tim-4 mAb RMT4-54, respectively (Figure 1D). These results suggest that Tim-3 as well as Tim-4 acts as a receptor for apoptotic cells.

To further address whether expression of Tim-3 could confer the ability to internalize or just bind apoptotic cells, we next used HEK293T cell reconstitution system because although ectopic expression of an authentic phagocytic receptor FcγRIII with FcRγ chain enabled this cell line to internalize IgG-opsonized bacteria, the expression of scavenger receptor-A (SR-A)[28] or paired Ig-like receptor-B (PIR-B),[29] which is the nonphagocytic receptor for bacteria, conferred the binding without significant internalization (not shown). As shown in

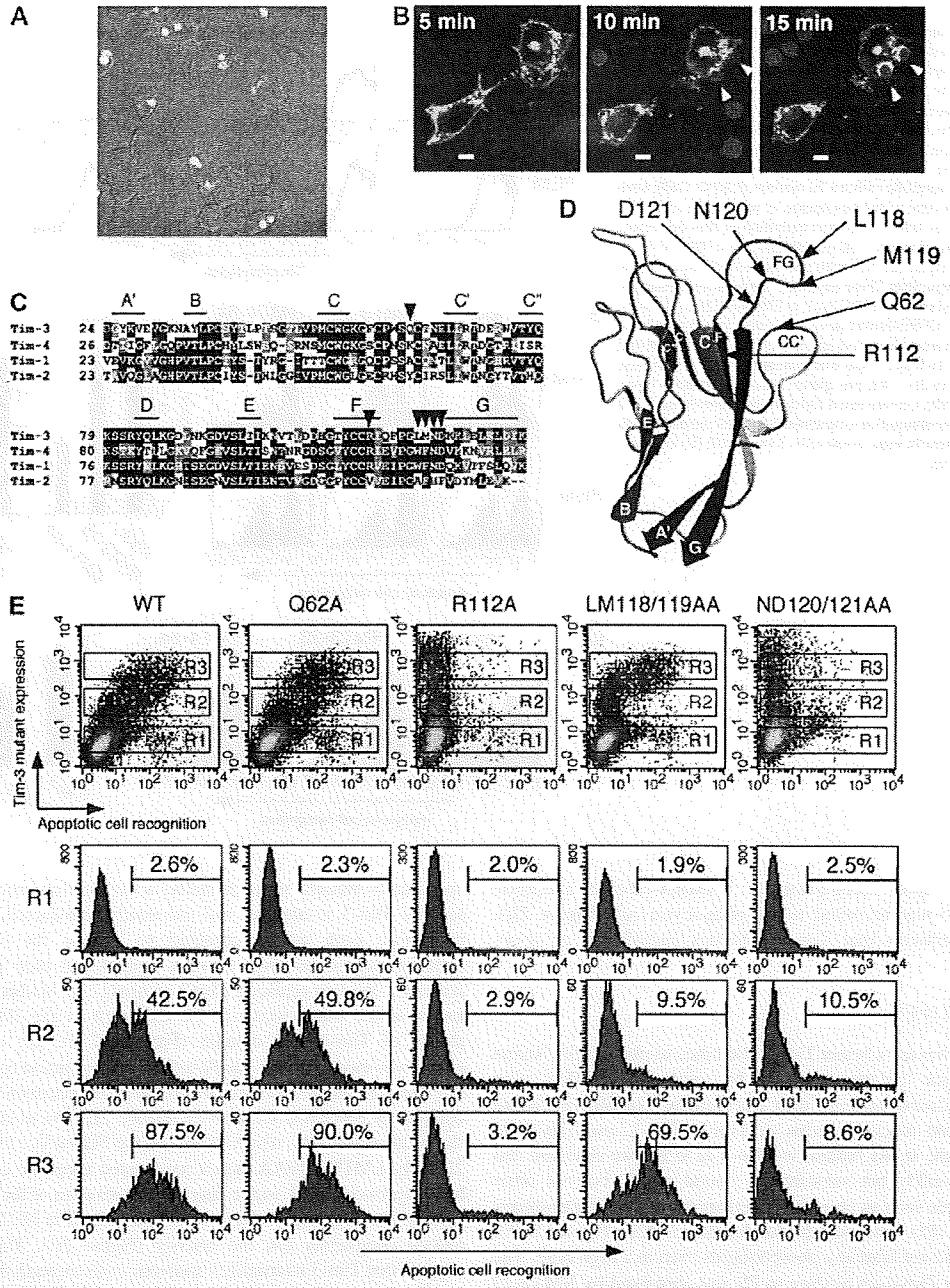

Figure 2. Tim-3 internalizes apoptotic cells through the FG loop in IgV domain. (A) HEK293T cells transiently expressing Tim-3 were cultured with CFSE-labeled apoptotic cells for 60 minutes at 37°C, and then cells were stained with biotinylated RMT3-23 and Alexa 594–avidin. (B) TAMRA-labeled apoptotic cells were added to HEK293T cells transiently expressing Tim-3-GFP under fluorescence microscope. Phagocytosis and Tim-3-GFP localization were analyzed at the indicated time points. White arrowheads indicate apoptotic cells internalized via Tim-3. White bars indicate 5 μm. (C) Alignment of IgV domain of Tim family molecules. The β-strands of Tim-3 were shown with lines. Mutated residues were indicated by red arrowheads. (D) Positions of mutated residues are indicated on 3-dimensional structure of Tim-3 IgV domain. The color of the protein main-chain is gradually changed along the sequence from blue (N-terminal) to red (C-terminal). (E) HEK293T cells transiently expressing wild-type or mutant Tim-3 were cultured with CFSE-labeled apoptotic cells for 60 minutes at 37°C, and then cells were stained with biotinylated RMT3-23 and PE-avidin. Recognition of apoptotic cells by gated HEK293T cells (R1; Tim-3$^-$, R2; Tim-3^{low}, R3; Tim-3^{high}) was analyzed by flow cytometry. Similar results were obtained in 2 (A,B) or 3 (E) independent experiments.

Figure 2A, Tim-3–positive cells efficiently internalized CFSE-labeled apoptotic cells, indicating that Tim-3 is a phagocytic receptor for apoptotic cells. Furthermore, we addressed Tim-3 localization upon initial contact with apoptotic cells. To visualize Tim-3, we generated an expression vector for Tim-3 fused at its C-terminus to green fluorescence protein (GFP), and then expressed this fusion receptor in HEK293T cells. Whereas Tim-3 was mostly expressed at the cell surface in resting

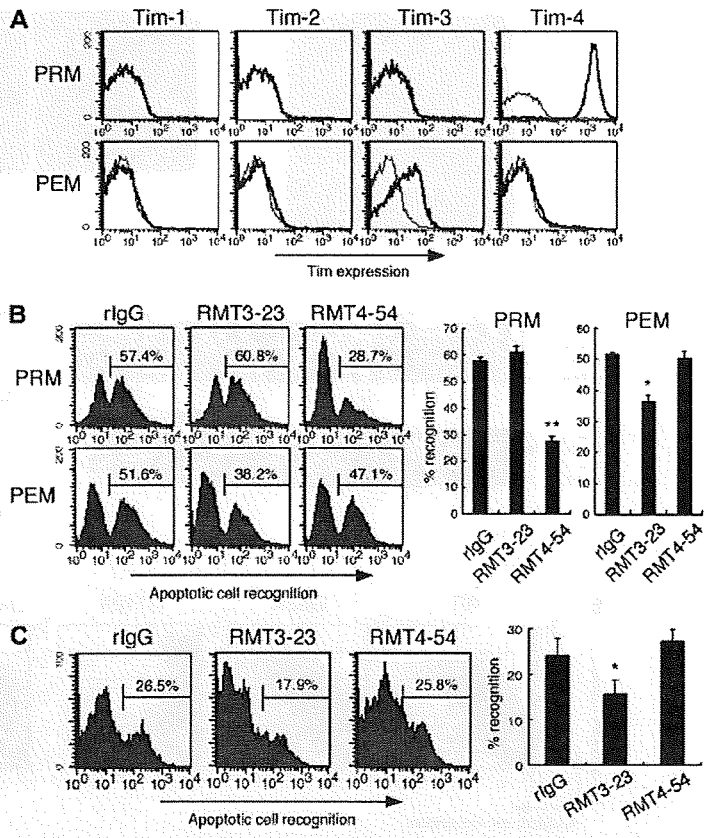

Figure 3. Tim-3 mediates phagocytosis of apoptotic cells by peritoneal exudate macrophages. (A) Peritoneal resident Mac1$^+$ cells (PRMs) and peritoneal exudate Mac1$^+$ cells (PEMs) were stained with biotinylated RMT1-17, RMT2-14, RMT3-23, or RMT4-54, followed by FITC-anti-CD11b mAb and PE-avidin (thick histograms); then CD11b$^+$ cells were analyzed by flow cytometry. Thin histograms indicate background staining with biotinylated control rat IgG2a. (B) Macrophages were pretreated with control rat IgG2a (rIgG), RMT3-23, or RMT4-54, and then cultured with CFSE-labeled apoptotic cells for 30 minutes at 37°C. Cells were stained with PE-Mac1, and percentage of recognition of CFSE-apoptotic cells by Mac1$^+$ cells was quantified by flow cytometry. Columns represent mean ± SD of triplicates (*$P < .05$; **$P < .01$ compared with rIgG). (C) Peritonitis was elicited by intraperitoneal injection of thioglycolate. Three days later, the mice were intraperitoneally injected with rIgG, RMT3-23, or RMT4-54 (200 μg/head), and then with CFSE-labeled apoptotic cells. Two hours later, peritoneal cells were harvested, and recognition of CFSE-labeled apoptotic cells by Mac1$^+$ cells was quantified by flow cytometry. The experiments (n = 4-5 per group) were performed 3 times independently with a similar result. Columns represent mean ± SD of 4 mice in a representative experiment (*$P < .05$ compared with rIgG). Similar results were obtained in 3 (A,C) or 2 (B) independent experiments.

conditions, upon recognition of TAMRA-labeled apoptotic cells, Tim-3 was recruited to the phagocytic cup (Figure 2B). This substantiates that Tim-3 mediates engulfment of apoptotic cells.

Tim-3 binds to PS

We next addressed whether Tim-3 also binds to phosphatidylserine (PS), a major "eat-me" signal,[1,2] by solid-phase ELISA using soluble Ig fusion proteins with extracellular domains including both IgV and mucin domains of Tim-2, Tim-3, and Tim-4. In addition to the strong binding of Tim-4-Ig to PS, we observed that Tim-3–Ig weakly but substantially bound to PS, but not other phospholipids such as phosphatidylethanolamine (PE), phosphatidylinositol (PI), and phosphatidylcholine (PC) (Figure S2A). Tim-2–Ig did not bind any phospholipids even at a high dose. The Tim-3–Ig or Tim-4–Ig binding to PS was abrogated by RMT3-23 or RMT4-54, respectively, in a dose-dependent manner (Figure S2B). These results indicate that Tim-3 recognizes PS, although the affinity is lower than that of Tim-4.

Tim-3 recognizes apoptotic cells through the FG loop in IgV domain

We next explored the Tim-3 recognition site of apoptotic cells. Recently, Santiago et al have revealed a crystal structure of Tim-4 and demonstrated that Tim-4 binds PS through the metal ion–dependent ligand binding site (MILIBS) in the FG loop, which is conserved in all Tim family members except Tim-2.[30] Thus, we specifically mutated some of amino acids locating around the FG loop of Tim-3 to alanine, and transiently transfected HEK293T cells with each mutant construct to address the relationship between expression level of each mutant and their phagocytic activities. We first replaced Gln62 or Arg112 to Ala because these amino acids, which locate in FG-CC′ cleft in the 3D structural model of Tim-3 IgV domain (Figure 2C,D), are critical for galectin-9–independent ligand binding.[31] Substitution of Gln62 did not alter the phagocytic activity, although substitution of Arg112 completely abrogated the activity (Figure 2E). We next addressed the putative MILIBS, which locates on the FG surface loop (Figure 2D). The LM118/119AA mutant recognized apoptotic cells only at high expression level, suggesting that substitution of these residues to both Ala weakened the activity (Figure 2E). The ND120/121AA mutant completely lost the activity (Figure 2E). These results suggest that Tim-3 internalizes apoptotic cells through the FG loop in IgV domain, and that at least in part galectin-9–independent ligand binding[31] might be linked to recognition of apoptotic cells.

Tim-3 and Tim-4 mediate phagocytosis of apoptotic cells by distinct macrophage subsets

We next examined the cell surface expression of Tim molecules on mouse primary macrophages, and their contribution to the phagocytosis of apoptotic cells. We found Tim-3 expression on peritoneal exudate Mac1$^+$ cells (PEMs), but not peritoneal resident Mac1$^+$ cells (PRMs) from naive mice (Figure 3A). In contrast, Tim-4 was highly expressed on PRMs, but not PEMs, which is consistent with

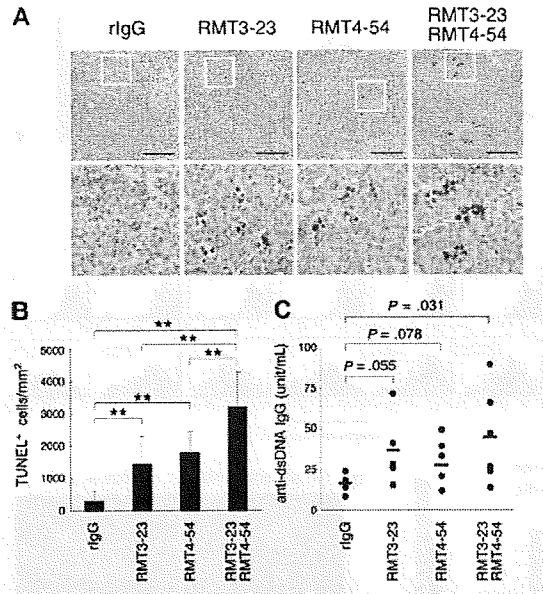

Figure 4. Involvement of Tim-3 in clearance of apoptotic cells in vivo. Mice (n = 4-6 per group) were treated with rIgG, RMT3-23, and/or RMT4-54 (200 μg each per mouse) twice a week for 4 weeks. (A) Apoptotic cells in paraffin-embedded spleen sections from these mice were detected by TdT-mediated dUTP nick-end labeling (TUNEL) method. Nuclei were counterstained with hematoxylin. Representative sections (top panels, ×20 magnification) were shown. Black bars indicate 100 μm. White squares mark the areas shown at a higher magnification (bottom panels, ×80). (B) The number of TUNEL-positive cells was counted in at least 10 randomly chosen follicles, represented as columns (**$P < .01$). (C) Anti-dsDNA antibody levels in serum were determined by ELISA. P values compared with rIgG are shown. Similar results were obtained in 2 independent experiments.

a previous report.[8] Neither Tim-1 nor Tim-2 was expressed on both types of macrophages (Figure 3A). This result prompted us to investigate whether these different types of macrophages use different Tim molecules to recognize apoptotic cells. As shown in Figure 3B, PRMs efficiently phagocytosed apoptotic cells, and this was significantly inhibited by RMT4-54, but not by RMT3-23. In contrast, phagocytosis of apoptotic cells by PEMs was significantly inhibited by RMT3-23, but not RMT4-54. These results suggest that although these macrophage subsets use MerTK and MFG-E8 to recognize and internalize apoptotic cells,[5,6,32] Tim-3 and Tim-4 also play a role in this process by PEMs and PRMs, respectively. Moreover, we used a mouse sterile peritonitis model to examine whether Tim-3 participates in the phagocytosis in vivo. As shown in Figure 3C, RMT3-23, but not RMT4-54, significantly inhibited the phagocytosis of apoptotic cells by peritoneal macrophages, suggesting that Tim-3 contributes to the phagocytosis of apoptotic cells in vivo.

Tim-3 is crucial for clearance of apoptotic cells in vivo

To evaluate the physiological role of Tim-3 and Tim-4 in vivo, we intraperitoneally injected RMT3-23 and/or RMT4-54 into C57BL/6 mice twice a week for 4 weeks, and stained apoptotic cells in various organs by terminal deoxynucleotidyl transferase–mediated deoxyuridine triphosphate nick-end labeling (TUNEL) method. In spleen follicles, treatment with either RMT3-23 or RMT4-54 significantly increased TUNEL$^+$ cells, and a remarkable increase was observed with the combination treatment (Figure 4A,B), whereas the administration of these mAbs did not increase the number of TUNEL$^+$ cells in the liver, pancreas, or brain (not shown).

It has been reported that an impairment of clearance of apoptotic cells induces autoantibody production.[5,33,34] Thus, we next measured serum level of autoantibodies in these mice. Consistent with a recent report,[8] blocking of Tim-4 by RMT4-54 induced anti-dsDNA antibodies (Figure 4C). We found that serum level of anti-dsDNA antibodies was also increased by RMT3-23 (Figure 4C). These results suggest that Tim-3 as well as Tim-4 participates in the clearance of apoptotic cells in vivo, and that the disabling of this system leads to autoantibody production.

Tim-3 mediates phagocytosis of apoptotic cells and cross-presentation by CD8$^+$ DCs in vitro

Because Tim-3 is involved in the clearance of apoptotic cells in not only inflammatory state (Figure 3C) but also steady state (Figure 4) in vivo, we further addressed the Tim-3 expression on several types of naive cells, and found that Tim-3 was highly expressed on peripheral blood monocytes and splenic DCs (Figure S3). Moreover, we noticed that the expression of Tim-3 on splenic CD8$^+$ DCs was approximately 3-fold higher than that on CD8$^-$ DCs (Figure 5A,B). Several groups have demonstrated that, in mouse spleen, CD8$^+$ DCs are uniquely able to recognize apoptotic cells, however, the receptor for apoptotic cells remains to be identified.[16-18] These reports prompted us to address whether Tim-3 plays a role for the recognition of apoptotic cells by this DC subset. Consistent with previous reports,[16,35] we observed that CD8$^+$ DCs recognized apoptotic cells more efficiently than CD8$^-$ DCs (Figure 5C). Interestingly, masking of Tim-3 by RMT3-23 inhibited approximately 50% recognition of apoptotic cells by CD8$^+$ DCs (Figure 5C,D), suggesting that CD8$^+$ DCs use Tim-3 to efficiently recognize apoptotic cells. Confocal microscopy revealed that, although Tim-3 is largely expressed at cell surface of naive CD8$^+$ DCs (Figure 5E left panel), upon recognition of apoptotic cells Tim-3 is recruited to the site of apoptotic cell apposition with the membrane (Figure 5E right panel), suggesting that Tim-3 mediates internalization of apoptotic cells by CD8$^+$ DCs.

Because CD8$^+$ DC is the splenic DC subset that plays a crucial role in cross-presentation,[15] we next performed cross-presentation study using OT-I T cells specific for $OVA_{257-264}$/H-2K^b. Consistent with previous reports,[15,16] we confirmed that CD8$^+$ DCs cultured with OVA-loaded, but not BSA-loaded, apoptotic cells could efficiently induce OT-I CD8$^+$ T-cell proliferation, and that OT-I cells did not directly respond to OVA-loaded apoptotic cells (Figure S4). Then, we investigated the requirement of Tim-3 for this cross-presentation. As shown in Figure 6A, we observed that CD8$^+$ DCs induced OT-I T-cell proliferation more vigorously than CD8$^-$ DCs, and that inhibition of the phagocytosis by RMT3-23 significantly abrogated the CD8$^+$ DC-induced OT-I cell proliferation. Moreover, we observed a remarkable reduction in IFN-γ production by RMT3-23 (Figure 6B), whereas both DC subsets loaded with $OVA_{257-264}$ peptides equally activated OT-I T cells, irrespective of masking Tim-3 by RMT3-23. Although splenic DCs express Tim-4 at low level, RMT4-54 did not inhibit the phagocytosis of apoptotic cells and the cross-presentation in vitro (Figures 5,6).

Tim-3 is crucial for phagocytosis of apoptotic cells and cross-presentation in vivo

We further addressed the contribution of Tim-3 to the phagocytosis of apoptotic cells and cross-presentation by CD8$^+$ DCs in vivo. It has been reported that intravenously injected apoptotic cells are taken up mainly by CD8$^+$ DCs in mouse spleen.[16,35] Consistently,

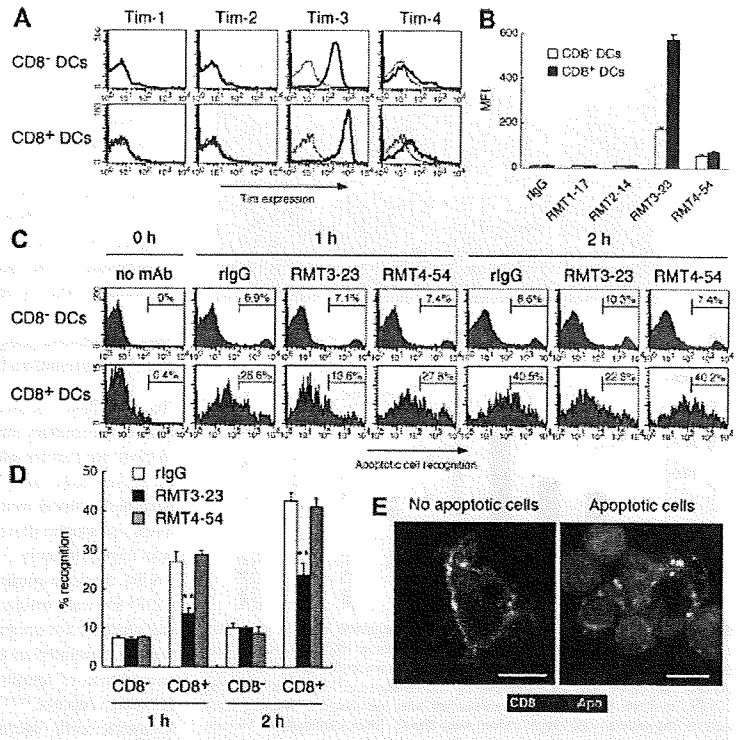

Figure 5. Tim-3 mediates phagocytosis of apoptotic cells by CD8⁺ DCs. (A) Low-density splenocytes were stained with biotinylated control rIgG2a (thin histograms), RMT1-17, RMT2-14, RMT3-23, or RMT4-54 (thick histograms), followed by PE-avidin, FITC–anti-CD11c mAb, and APC–anti-CD8α mAb; then Tim expression on CD8⁻CD11c⁺ or CD8⁺CD11c⁺ cells was analyzed by flow cytometry. The average of mean fluorescence intensity (MFI) ± SD of triplicates is represented in panel B. (C) Purified splenic CD11c⁺ cells prestained with APC–anti-CD8α mAb were treated with rIgG, RMT3-23, or RMT4-54, and then cultured with TAMRA-labeled apoptotic cells at 37°C. After the indicated time period, cells were stained with FITC–anti-CD11c mAb, and percentage recognition of TAMRA-labeled apoptotic cells by CD8⁻CD11c⁺ or CD8⁺CD11c⁺ cells was quantified by flow cytometry. Columns represent mean ± SD of triplicates in panel D (**$P < .01$ compared with rIgG). (E) (Left panel) Purified splenic CD11c⁺ cells were stained with Alexa 647–anti-CD8 mAb and Alexa 594–RMT3-23. (Right panel) Purified splenic CD11c⁺ cells prestained with Alexa 647–anti-CD8 mAb were cultured with CFSE-labeled apoptotic cells for 60 minutes at 37°C, and then cells were stained with Alexa 594–RMT3-23. Cells were analyzed by confocal microscopy. White bars indicate 5 μm. Similar results were obtained in 3 (A-D) or 2 (E) independent experiments.

we also observed that CD8⁺ DCs efficiently recognized CFSE-labeled apoptotic cells 1 hour after intravenous injection (Figure 7A,B). Interestingly, the recognition was significantly abrogated by RMT3-23. To rule out the possibility that binding of RMT3-23 to FcR on DCs might affect phagocytosis of apoptotic cells, we pretreated mice with anti-FcR (2.4G2). As shown in Figure S5C, 2.4G2 did not affect the blocking activity of RMT3-23. Moreover, we prepared $F(ab')_2$ fragments of RMT3-23, and observed that the $F(ab')_2$ fragments did not lose the blocking effect (Figure S5), indicating that the blocking effect of RMT3-23 is not mediated through FcRs. These results suggest that Tim-3 is crucial for the recognition of apoptotic cells by CD8⁺ DCs in vivo.

To study cross-presentation of apoptotic cell–associated antigens in vivo, we transferred CFSE-labeled OT-I T cells into C57BL/6 mice, and then 1 day later, we primed these mice with OVA-loaded dying splenocytes. Two days after the priming, we observed that OT-I cells proliferated vigorously in spleen (Figure 7C,D), although OT-I cells did not proliferate in unprimed mouse spleen, indicating that dying cell-associated OVA antigens were taken up by splenic CD8⁺ DCs and cross-presented to OT-I cells. Consistent with a crucial role of Tim-3 for the uptake of apoptotic cells by CD8⁺ DCs (Figure 7A,B), the proliferation of OT-I cells was also significantly reduced by RMT3-23, but not RMT4-54 (Figure 7C,D). These results suggest that Tim-3 plays a crucial role in phagocytosis of apoptotic cells and subsequent cross-presentation by CD8⁺ DCs in vivo.

Discussion

Phagocytes such as macrophages and DCs efficiently recognize and engulf apoptotic cells to maintain the peripheral tolerance. In this study, we demonstrate that Tim-3 mediates phagocytosis of apoptotic cells by PEMs and CD8⁺ DCs, and that disabling of the Tim-3 function in vivo induces autoantibody production. Likewise, several studies have shown that impairment of the clearance of apoptotic cells causes autoantibody production,[5,8,34] however, the mechanism for the elicited immune response to dying cells remains to be elucidated. As the possible explanation, delay or impairment of clearance of apoptotic cells by macrophages causes secondary necrotic cells releasing intracellular contents, which could be endogenous "danger signal" activating immune system.[1] However, chronic administration of apoptotic thymocytes to syngeneic mice induces more remarkable level of autoantibody production than that of the same dose of nonapoptotic cell lysate,[36] suggesting that autoantibody production in response to dying cells could not be explained simply by the exposure of the intracellular contents. It has also been reported that, in mice, CD8⁺ DC subset is unique in its ability to recognize apoptotic cells and cross-present dying cell-associated antigens.[15,16] It is considered that, in steady state, cross-presentation of dying cell-associated self-antigens by CD8⁺ DCs induces autoreactive CD8⁺ T-cell proliferation abortively, subsequently resulting in their deletion, which is important to maintain peripheral tolerance.[10,13,14] Taken together, Tim-3–mediated phagocytosis of apoptotic cells by CD8⁺ DCs may be linked to peripheral tolerance, and a loss of Tim-3 function in DCs may exacerbate autoimmunity. Consistent with this hypothesis, we and others have reported that Tim-3 negatively regulates Th1-mediated inflammatory diseases such as EAE, type I diabetes, and aGVHD, and promotes tolerance induction.[21-23]

Alternatively, however, upon being activated by anti-CD40 mAb, endogenous danger signals such as heat shock proteins and uric acid, or pathogen-associated molecular patterns (PAMPs) such as LPS and CpG, DCs turn to cross-prime CD8⁺ T cells to generate

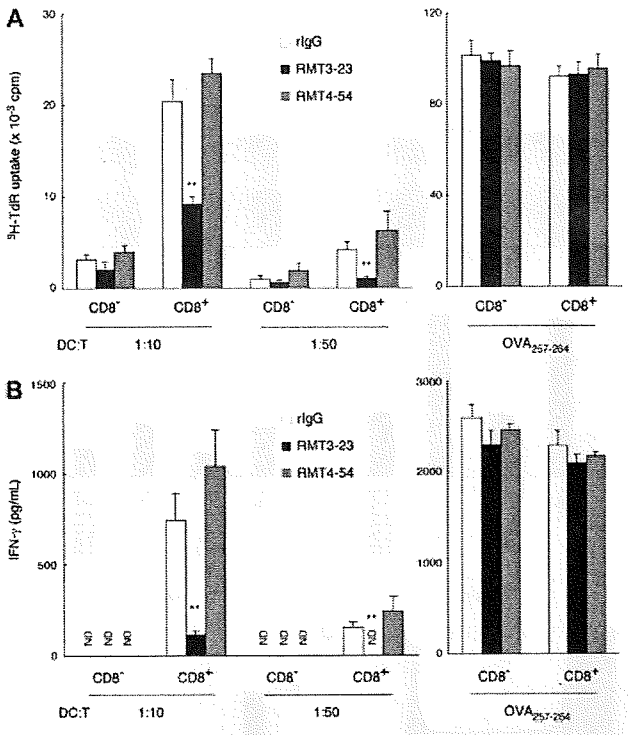

Figure 6. Tim-3–mediated phagocytosis of apoptotic cells is crucial for the cross-presentation by CD8$^+$ DCs. (A) Purified CD8$^-$CD11c$^+$ or CD8$^+$CD11c$^+$ splenic DCs were pretreated with rIgG (white histograms), RMT3-23 (black histograms), or RMT4-54 (gray histograms) and then cultured with OVA-loaded apoptotic cells. After 2 hours, both DC subsets were purified again to remove dead cells, and then cocultured with OT-I CD8$^+$ T cells at the indicated ratio. For the direct presentation, both DC subsets preincubated with $OVA_{257-264}$ peptide (1 nM) in the presence of rIgG, RMT3-23, or RMT4-54 were cocultured with OT-I CD8$^+$ T cells at a 1:10 (DC/T) ratio. [^{3}H]thymidine (^{3}H-TdR) uptake was measured at 48 to 60 hours. (B) Production of IFN-γ in the culture supernatant at 48 hours after addition of OT-I CD8$^+$ T cells was measured by ELISA. Columns represent mean ± SD of triplicates (**$P < .01$ compared with rIgG). ND indicates not detectable. Similar results were obtained in 3 independent experiments (A,B).

effector cells.[10,12] Given that Tim-3 is crucial for IFN-γ production in cross-presentation and that Tim-3 is expressed on sterile inflammatory macrophages, Tim-3 may promote induction of effector CD8$^+$ T-cell proliferation and functional memory under pathological conditions. Indeed, Anderson et al have recently reported that Tim-3 expressed on DCs exacerbates a Th1-type autoimmune disease EAE.[25] Although Tim-3 has been reported to have multiple functions,[21-23] it would be important to further address whether this novel function of Tim-3 is linked to immune tolerance or activation under pathological conditions.

It remains unclear why CD8$^-$ DCs are not able to engulf apoptotic cells efficiently, although this DC subset expresses Tim-3. One possibility is that the phagocytic activity may be determined by relative expression level of receptors for "eat-me" signals and "don't eat-me" signals. Although we observed that expression level of Tim-3 on CD8$^+$ DCs is approximately 3-fold higher than that on CD8$^-$ DCs, it has been reported that signal-regulatory protein (SIRP)α, a receptor for "don't eat-me" signal,[37] is much more highly expressed on CD8$^-$ DCs than CD8$^+$ DCs.[38] Taken together, a high expression of Tim-3 may be required for the phagocytosis by DCs, and/or SIRPα may neutralize Tim-3 function on CD8$^-$ DCs. Moreover, phagocytic activity of each cell type may be determined not only by expression level of the phagocytic receptor, but also cell-intrinsic phagocytic machinery such as cytoskeletal architecture. Indeed, Tim-3 as well as Tim-1 is expressed on activated T cells,[24,39] but these T cells are not able to recognize apoptotic cells.

In this study, ectopic expression of Tim-3 enabled HEK293T cells to engulf whole apoptotic cells. However, Miyanishi et al could not observe the phagocytic activity of Tim-3 expressed on NIH3T3 cells based on their engulfment assay, which quantified nuclear DNA degradation of apoptotic cells engulfed by NIH3T3 expressing Tim-3 and DNase II.[8] To address this discrepancy, we also generated NIH3T3 cells expressing Tim-3, and did not observe the ability of Tim-3 to mediate engulfment of whole apoptotic cells, although we did observe the ability of Tim-3 to incorporate CFSE-labeled apoptotic cell debris (Figure S6). The reason why Tim-3 expressed on NIH3T3 cells is not able to efficiently phagocytose apoptotic cells remains to be elucidated. We cannot rule out the possibility that Tim-3 may recognize apoptotic cells in cooperation with some coreceptor, which may be expressed on HEK293T cells, macrophages, and CD8$^+$ DCs, but not NIH3T3 cells or CD8$^-$ DCs. Likewise, it has been reported that although gene targeting of MerTK receptor results in remarkable defect of phagocytosis of apoptotic cells by macrophages,[5] the receptor requires coexpression of $\alpha_V\beta_5$ integrin to enable NIH3T3 cells to recognize apoptotic cells.[40] Although we did observe PS binding of Tim-3 by solid-phase ELISA, Miyanishi et al failed to observe this by PIP–strip binding assay.[8] This discrepancy is probably due to a difference in assay sensitivity. Given that the affinity of Tim-3 to PS is much lower than that of Tim-4, Tim-3 might bind not only PS but also some other ligand to phagocytose apoptotic cells. Further studies are needed to elucidate the complexity of phagocytosis.

We show here a crucial role of Tim-3 for clearance of apoptotic cells in vivo and differential expression profile of phagocytic Tim molecules, suggesting that the pathophysiological roles of each Tim molecule appear to be different. Because Tim-1 is expressed on epithelial cells but not professional phagocytes, Tim-1 may contribute to remodeling of injured epithelia.[9] Tim-4 is highly expressed on PRMs, and contributes to the phagocytosis of apoptotic cells during physiological tissue turnover.[8] Our findings highlight Tim-3 as the phagocytic receptor responsible for cross-presentation by CD8$^+$ DCs. This novel function of Tim-3 opens the door to new therapeutic approaches to combat infections, cancers, and autoimmune diseases.

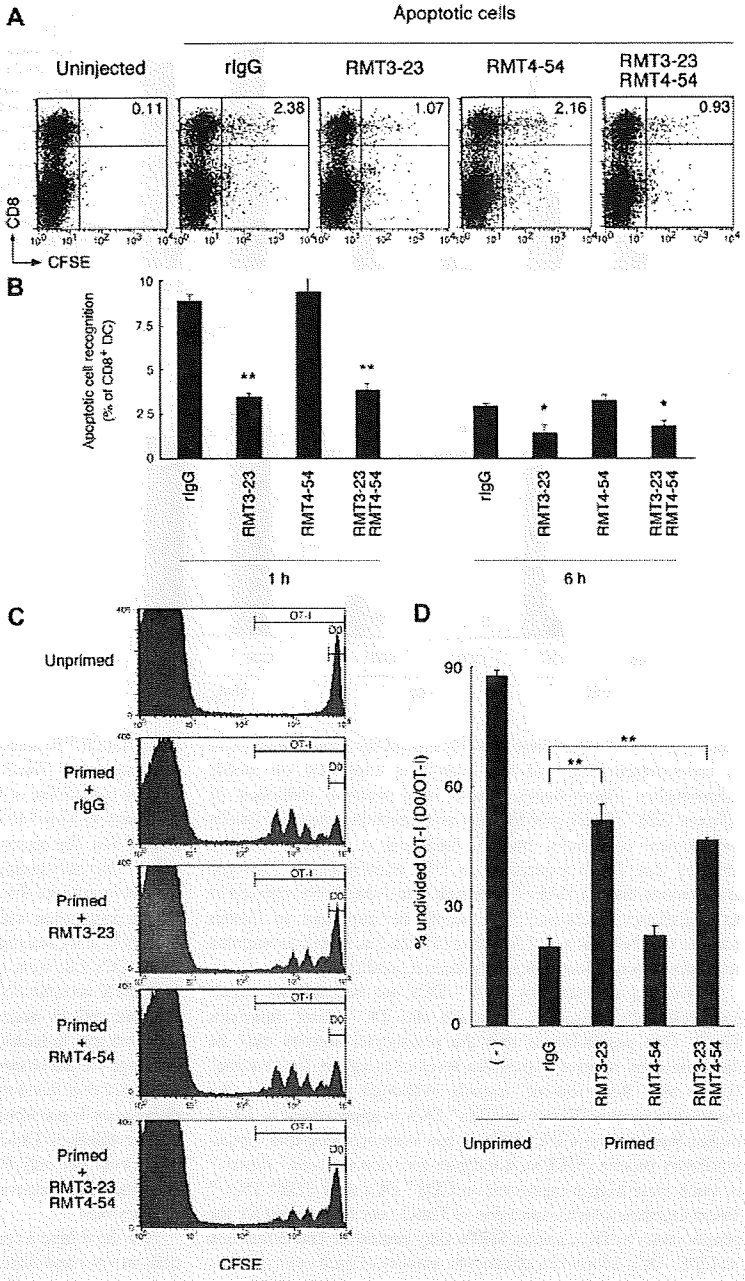

Figure 7. Tim-3 is crucial for the phagocytosis of apoptotic cells and cross-presentation in vivo. (A) Mice (n = 3 per group) were intravenously injected with the indicated mAb (200 μg each per head), and then 2 hours later with CFSE-labeled apoptotic splenocytes (2×10^7 per head). One hour later, collagenase-digested splenocytes were harvested, and recognition of CFSE-labeled apoptotic cells by splenic $CD11c^+$ cells was analyzed by flow cytometry. Numbers indicate percentage of cells in top right quadrants. (B) Collagenase-digested splenocytes were harvested from mice treated as described in panel A at indicated time points, and recognition of apoptotic cells by splenic $CD8^+$ DCs was analyzed by flow cytometry. Percentage recognition of CFSE-labeled apoptotic cells by $CD8^+$ DCs (percentage $CFSE^+CD8^+CD11c^-$ cells/percentage $CD8^-CD11c^+$ cells × 100) was calculated. Columns represent mean ± SD of triplicates ($^*P < .05$; $^{**}P < .01$ compared with rIgG). Similar results were obtained in 3 independent experiments. (C) CFSE-labeled OT-I $CD8^+$ T cells (2×10^6 per head) were intravenously transferred into B6 mice (n = 3 per group). The next day, mice were intravenously injected with the indicated mAb (200 μg each per head), and then 2 hours later primed with OVA-loaded apoptotic cells (10^7 per head). Two days later, whole splenocytes were harvested, and CFSE intensity of $CD8^+V\alpha2^+$ OT-I cells was analyzed by flow cytometry. Percentage of undivided cells in total OT-I cells (D0 per OT-I in C) was calculated, and mean ± SD of triplicates was shown in panel D ($^{**}P < .01$ compared with rIgG). Similar results were obtained in 3 independent experiments.

Acknowledgments

We thank Drs William R. Heath for OT-I mice, Sachiko Hirose for aged (NZB × NZW) F1 mice serum, and Toshio Kitamura for pMXs-IRES-puro vector. We also thank Dr Tamami Sakanishi for cell sorting.

This work was supported by the Grants-in-Aid for Scientific Research from the Japanese Ministry of Education, Culture, Sports, Science and Technology (Tokyo, Japan), and by a grant from "High-Tech Research Center" Project for Private Universities: matching fund subsidy from the Ministry of Education, Culture, Sports, Science and Technology (Tokyo, Japan).

Authorship

Contribution: M.N. designed and performed experiments; H.A. provided vital reagents; H.A., Y.K., and M.H. discussed experimental strategy and performed experiments; K.T. designed and discussed experimental strategy; M.A., H.Y., and K.O. supervised

experiments and discussed the experimental strategy; M.N. wrote the paper; and K.T. and H.Y. edited the paper.

Conflict-of-interest disclosure: The authors declare no competing financial interests.

Correspondence: Masafumi Nakayama, Department of Immunology, Juntendo University School of Medicine, 2-1-1 Hongo, Bunkyo-ku, Tokyo 113-8421, Japan; e-mail: nakayama@juntendo.ac.jp.

References

1. Savill J, Dransfield I, Gregory C, Haslett C. A blast from the past: clearance of apoptotic cells regulates immune responses. Nat Rev Immunol. 2002;2:965-975.
2. Henson PM, Hume DA. Apoptotic cell removal in development and tissue homeostasis. Trends Immunol. 2006;27:244-250.
3. Cohen JJ, Duke RC, Fadok VA, Sellins KS. Apoptosis and programmed cell death in immunity. Annu Rev Immunol. 1992;10:267-293.
4. Ravichandran KS, Lorenz U. Engulfment of apoptotic cells: signals for a good meal. Nat Rev Immunol. 2007;7:964-974.
5. Scott RS, McMahon EJ, Pop SM, et al. Phagocytosis and clearance of apoptotic cells is mediated by MER. Nature. 2001;411:207-211.
6. Hanayama R, Tanaka M, Miwa K, Shinohara A, Iwamatsu A, Nagata S. Identification of a factor that links apoptotic cells to phagocytes. Nature. 2002;417:182-187.
7. Park D, Tosello-Trampont AC, Elliott MR, et al. BAI1 is an engulfment receptor for apoptotic cells upstream of the ELMO/Dock180/Rac module. Nature. 2007;450:430-434.
8. Miyanishi M, Tada K, Koike M, Uchiyama Y, Kitamura T, Nagata S. Identification of Tim4 as a phosphatidylserine receptor. Nature. 2007;450:435-439.
9. Kobayashi N, Karisola P, Pena-Cruz V, et al. TIM-1 and TIM-4 glycoproteins bind phosphatidylserine and mediate uptake of apoptotic cells. Immunity. 2007;27:927-940.
10. Heath WR, Belz GT, Behrens GM, et al. Cross-presentation, dendritic cell subsets, and the generation of immunity to cellular antigens. Immunol Rev. 2004;199:9-26.
11. Kurts C, Kosaka H, Carbone FR, Miller JF, Heath WR. Class I-restricted cross-presentation of exogenous self-antigens leads to deletion of autoreactive CD8(+) T cells. J Exp Med. 1997;186:239-245.
12. Liu K, Iyoda T, Saternus M, Kimura Y, Inaba K, Steinman RM. Immune tolerance after delivery of dying cells to dendritic cells in situ. J Exp Med. 2002;196:1091-1097.
13. Redmond WL, Sherman LA. Peripheral tolerance of CD8 T lymphocytes. Immunity. 2005;22:275-284.
14. Luckashenak N, Schroeder S, Endt K, et al. Constitutive crosspresentation of tissue antigens by dendritic cells controls CD8+ T cell tolerance in vivo. Immunity. 2008;28:521-532.
15. den Haan JM, Lehar SM, Bevan MJ. CD8(+) but not CD8(−) dendritic cells cross-prime cytotoxic T cells in vivo. J Exp Med. 2000;192:1685-1696.
16. Iyoda T, Shimoyama S, Liu K, et al. The CD8+ dendritic cell subset selectively endocytoses dying cells in culture and in vivo. J Exp Med. 2002;195:1289-1302.
17. Schulz O, Pennington DJ, Hodivala-Dilke K, Febbraio M, Reis e Sousa C. CD36 or alphavbeta3 and alphavbeta5 integrins are not essential for MHC class I cross-presentation of cell-associated antigen by CD8 alpha+ murine dendritic cells. J Immunol. 2002;168:6057-6065.
18. Belz GT, Vremec D, Febbraio M, et al. CD36 is differentially expressed by CD8+ splenic dendritic cells but is not required for cross-presentation in vivo. J Immunol. 2002;168:6066-6070.
19. Monney L, Sabatos CA, Gaglia JL, et al. Th1-specific cell surface protein Tim-3 regulates macrophage activation and severity of an autoimmune disease. Nature. 2002;415:536-541.
20. Anderson AC, Anderson DE. TIM-3 in autoimmunity. Curr Opin Immunol. 2006;18:655-659.
21. Sabatos CA, Chakravarti S, Cha E, et al. Interaction of Tim-3 and Tim-3 ligand regulates T helper type 1 responses and induction of peripheral tolerance. Nat Immunol. 2003;4:1102-1110.
22. Sánchez-Fueyo A, Tian J, Picarella D, et al. Tim-3 inhibits T helper type 1-mediated auto- and alloimmune responses and promotes immunological tolerance. Nat Immunol. 2003;4:1093-1101.
23. Oikawa T, Kamimura Y, Akiba H, et al. Preferential involvement of Tim-3 in the regulation of hepatic CD8+ T cells in murine acute graft-versus-host disease. J Immunol. 2006;177:4281-4287.
24. Zhu C, Anderson AC, Schubart A, et al. The Tim-3 ligand galectin-9 negatively regulates T helper type 1 immunity. Nat Immunol. 2005;6:1245-1252.
25. Anderson AC, Anderson DE, Bregoli L, et al. Promotion of tissue inflammation by the immune receptor Tim-3 expressed on innate immune cells. Science. 2007;318:1141-1143.
26. Xiu Y, Nakamura K, Abe M, et al. Transcriptional regulation of Fcgr2b gene by polymorphic promoter region and its contribution to humoral immune responses. J Immunol. 2002;169:4340-4346.
27. Li M, Davey GM, Sutherland RM, et al. Cell-associated ovalbumin is cross-presented much more efficiently than soluble ovalbumin in vivo. J Immunol. 2001;166:6099-6103.
28. Peiser L, Gough PJ, Kodama T, Gordon S. Macrophage class A scavenger receptor-mediated phagocytosis of Escherichia coli: role of cell heterogeneity, microbial strain, and culture conditions in vitro. Infect Immun. 2000;68:1953-1963.
29. Nakayama M, Underhill DM, Petersen TW, et al. Paired Ig-like receptors bind to bacteria and shape TLR-mediated cytokine production. J Immunol. 2007;178:4250-4259.
30. Santiago C, Ballesteros A, Martinez-Munoz L, et al. Structures of T cell immunoglobulin mucin protein 4 show a metal-Ion-dependent ligand binding site where phosphatidylserine binds. Immunity. 2007;27:941-951.
31. Cao E, Zang X, Ramagopal UA, et al. T cell immunoglobulin mucin-3 crystal structure reveals a galectin-9-independent ligand-binding surface. Immunity. 2007;26:311-321.
32. Hu B, Jennings JH, Sonstein J, et al. Resident murine alveolar and peritoneal macrophages differ in adhesion of apoptotic thymocytes. Am J Respir Cell Mol Biol. 2004;30:687-693.
33. Asano K, Miwa M, Miwa K, et al. Masking of phosphatidylserine inhibits apoptotic cell engulfment and induces autoantibody production in mice. J Exp Med. 2004;200:459-467.
34. Hanayama R, Tanaka M, Miyasaka K, et al. Autoimmune disease and impaired uptake of apoptotic cells in MFG-E8-deficient mice. Science. 2004;304:1147-1150.
35. Schnorrer P, Behrens GM, Wilson NS, et al. The dominant role of CD8+ dendritic cells in cross-presentation is not dictated by antigen capture. Proc Natl Acad Sci U S A. 2006;103:10729-10734.
36. Mevorach D, Zhou JL, Song X, Elkon KB. Systemic exposure to irradiated apoptotic cells induces autoantibody production. J Exp Med. 1998;188:387-392.
37. Gardai SJ, McPhillips KA, Frasch SC, et al. Cell-surface calreticulin initiates clearance of viable or apoptotic cells through trans-activation of LRP on the phagocyte. Cell. 2005;123:321-334.
38. Lahoud MH, Proietto AI, Gartlan KH, et al. Signal regulatory protein molecules are differentially expressed by CD8- dendritic cells. J Immunol. 2006;177:372-382.
39. de Souza AJ, Oriss TB, O'Malley KJ, Ray A, Kane LP. T cell Ig and mucin 1 (TIM-1) is expressed on in vivo-activated T cells and provides a costimulatory signal for T cell activation. Proc Natl Acad Sci U S A. 2005;102:17113-17118.
40. Wu Y, Singh S, Georgescu MM, Birge RB. A role for Mer tyrosine kinase in alphavbeta5 integrin-mediated phagocytosis of apoptotic cells. J Cell Sci. 2005;118:539-553.

Differential Roles of Interleukin-17A and -17F in Host Defense against Mucoepithelial Bacterial Infection and Allergic Responses

Harumichi Ishigame,[1] Shigeru Kakuta,[1] Takeshi Nagai,[2] Motohiko Kadoki,[1] Aya Nambu,[1] Yutaka Komiyama,[1] Noriyuki Fujikado,[1] Yuko Tanahashi,[1] Aoi Akitsu,[1] Hayato Kotaki,[1] Katsuko Sudo,[1,5] Susumu Nakae,[1,3] Chihiro Sasakawa,[2] and Yoichiro Iwakura[1,4,*]
[1]Center for Experimental Medicine
[2]Department of Microbiology and Immunity
[3]Frontier Research Initiative
The Institute of Medical Science, The University of Tokyo, 4-6-1 Shirokanedai, Minato-ku, Tokyo, 108-8639, Japan
[4]Core Research for Evolutional Science and Technology (CREST), Japan Science and Technology Agency, Saitama 332-0012, Japan
[5]Present address: Animal Research Center, Tokyo Medical University, 6-1-1 Shinjyuku, Shinjyuku-ku, Tokyo 160-8402, Japan
*Correspondence: iwakura@ims.u-tokyo.ac.jp
DOI 10.1016/j.immuni.2008.11.009

SUMMARY

Interleukin-17A (IL-17A) is a cytokine produced by T helper 17 (Th17) cells and plays important roles in the development of inflammatory diseases. Although IL-17F is highly homologous to IL-17A and binds the same receptor, the functional roles of this molecule remain largely unknown. Here, we demonstrated with *Il17a*$^{-/-}$, *Il17f*$^{-/-}$, and *Il17a*$^{-/-}$*Il17f*$^{-/-}$ mice that IL-17F played only marginal roles, if at all, in the development of delayed-type and contact hypersensitivities, autoimmune encephalomyelitis, collagen-induced arthritis, and arthritis in *Il1rn*$^{-/-}$ mice. In contrast, both IL-17F and IL-17A were involved in host defense against mucoepithelial infection by *Staphylococcus aureus* and *Citrobacter rodentium*. IL-17A was produced mainly in T cells, whereas IL-17F was produced in T cells, innate immune cells, and epithelial cells. Although only IL-17A efficiently induced cytokines in macrophages, both cytokines activated epithelial innate immune responses. These observations indicate that IL-17A and IL-17F have overlapping yet distinct roles in host immune and defense mechanisms.

INTRODUCTION

Naive CD4$^+$ T cells are categorized into several helper T (Th) cell subsets, including Th1 and Th2 cells, on the basis of their cytokine production profiles and effector functions. Recently, Th17 cells that preferentially produce interleukin-17A (IL-17A), IL-17F, IL-21, and IL-22 were identified in mice (McGeachy and Cua, 2008; Ouyang et al., 2008). Th17 cell differentiation is induced by TGF-β plus IL-6 (Bettelli et al., 2006; Mangan et al., 2006; Veldhoen et al., 2006a) or IL-21 (Korn et al., 2007; Nurieva et al., 2007; Zhou et al., 2007) and accelerated by the coordinated activities of IL-1 and TNF (Veldhoen et al., 2006a). IL-23 is required for the growth, survival, and effector functions of Th17 cells and promotes IL-17A and IL-17F production by this T cell subset (Veldhoen et al., 2006a; Zhou et al., 2007).

IL-17F and IL-17A are highly homologous members of the IL-17 protein family and are encoded by genes that are located nearby each other in both humans and mice (Kawaguchi et al., 2004; Kolls and Linden, 2004; Weaver et al., 2007). It has been reported that IL-17A and IL-17F may bind the same receptor complexes consisting of IL-17RA and IL-17RC (Toy et al., 2006; Zheng et al., 2008), suggesting that these cytokines have similar biological functions. Consistent with this notion, both IL-17A and IL-17F induce the production of antimicrobial peptides (defensins), cytokines (IL-6, G-CSF, GM-CSF), and chemokines (CXCL1, CXCL2, CXCL5), as well as enhance granulopoiesis and neutrophil recruitment (Kawaguchi et al., 2004; Kolls and Linden, 2004; Weaver et al., 2007). Overexpression of IL-17F or IL-17A in the lungs leads to increased proinflammatory cytokine and chemokine expression, resulting in inflammation associated with neutrophil infiltration (Hurst et al., 2002; Oda et al., 2005; Park et al., 2005; Yang et al., 2008).

Several lines of evidence have established that the IL-23–IL-17A signaling axis rather than the IL-12–IFN-γ signaling axis is responsible for the development of autoimmune diseases such as experimental autoimmune encephalomyelitis (EAE), collagen-induced arthritis (CIA), and inflammatory bowel disease (IBD), as well as allergic diseases such as contact hypersensitivity (CHS) and delayed-type hypersensitivity (DTH) in mice (McGeachy and Cua, 2008; Oboki et al., 2008). Recent studies suggest that Th17 cells are also involved in the host defense against infection, because antigen-presenting cells (APCs) stimulated with such microbial products as lipopolysaccharide (LPS), peptidoglycans, and zymosan produce a large amount of IL-23, resulting in the development of Th17 cells (LeibundGut-Landmann et al., 2007; van Beelen et al., 2007; Veldhoen et al., 2006b). Furthermore, *Il17ra*$^{-/-}$ mice and/or *Il23a*$^{-/-}$ mice are more susceptible to *Klebsiella pneumoniae* in the lungs (Happel et al., 2005) and *Citrobacter rodentium* in the intestines (Mangan et al., 2006; Zheng et al., 2008). However, the relative contributions of IL-17A and IL-17F to autoimmune and allergic diseases as well as host defense processes remain to be elucidated.

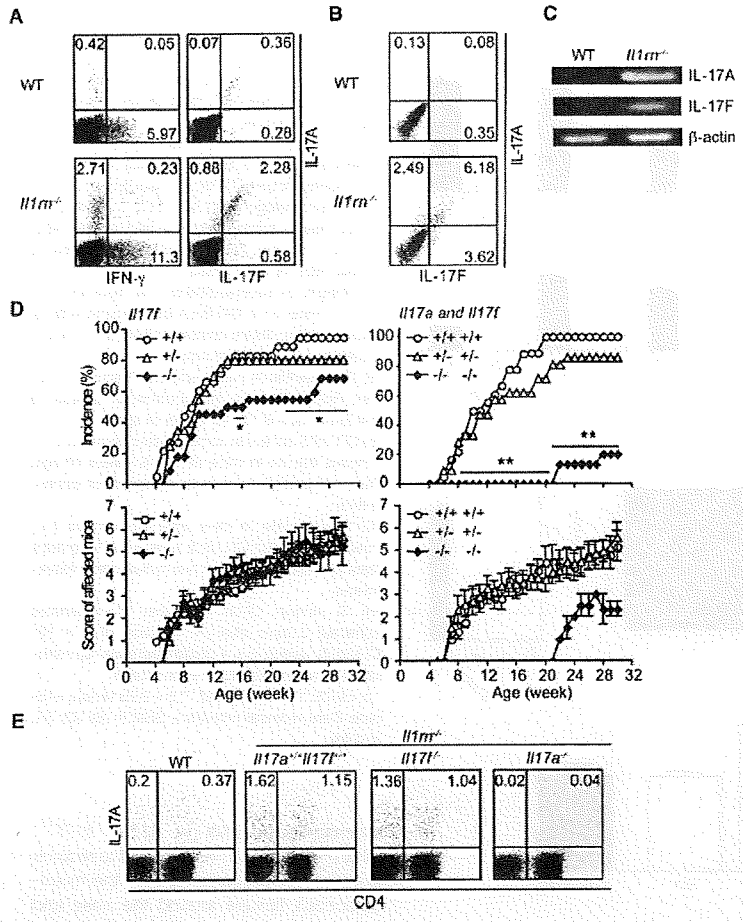

Figure 1. IL-17F Contributes to the Development of Spontaneous Autoimmune Arthritis in *Il1rn*$^{-/-}$ Mice

(A) Profiles of intracellular IL-17F, IL-17A, and IFN-γ expression in LN cells from wild-type and arthritic *Il1rn*$^{-/-}$ mice stimulated with PMA and ionomycin in vitro.

(B) Profiles of intracellular IL-17F, IL-17A, and IFN-γ expression in cells from the ankle joints of wild-type and arthritic *Il1rn*$^{-/-}$ mice stimulated with PMA and ionomycin.

(C) Expression of IL-17A and IL-17F mRNA in the joints of arthritic *Il1rn*$^{-/-}$ mice.

(D) Arthritis incidence and severity scores in *Il1rn*$^{-/-}$ mice. Left panels: open circles represent *Il17f*$^{+/+}$, open triangles represent *Il17f*$^{+/-}$, and closed diamonds represent *Il17f*$^{-/-}$ mice on an *Il1rn*$^{-/-}$ background; right panels: open circles represent *Il17a*$^{+/+}$ *Il17f*$^{+/+}$, open triangles represent *Il17a*$^{+/-}$*Il17f*$^{+/-}$, and closed diamonds represent *Il17a*$^{-/-}$*Il17f*$^{-/-}$ mice on an *Il1rn*$^{-/-}$ background (n = 15–22/group). *, $p < 0.05$ and **, $p < 0.01$ versus *Il17f*$^{+/+}$ or *Il17a*$^{+/+}$*Il17f*$^{+/+}$ mice determined with χ^2 tests.

(E) Intracellular IL-17A expression in LN cells from wild-type, *Il17a*$^{+/+}$*Il17f*$^{+/+}$*Il1m*$^{-/-}$, *Il17f*$^{-/-}$ *Il1m*$^{-/-}$, and *Il17a*$^{-/-}$*Il1m*$^{-/-}$ mice stimulated with PMA and ionomycin.

Data are representative of two (C and E) or three (A and B) independent experiments.

In this study, we discriminated between the functions of IL-17F and IL-17A in immune responses and host defense mechanisms directed against bacterial infection. To accomplish this, we have generated mice lacking IL-17F (*Il17f*$^{-/-}$) or both IL-17A and IL-17F (*Il17a*$^{-/-}$*Il17f*$^{-/-}$), which were used together with previously generated *Il17a*$^{-/-}$ mice (Nakae et al., 2002), and shown that IL-17A and IL-17F play distinct roles in the development of T cell-mediated inflammation and immune responses against bacterial infection.

RESULTS

IL-17F Contributes to the Development of Arthritis in IL-1 Receptor Antagonist-Deficient Mice

To elucidate the functional differences between IL-17F and IL-17A in the immune system, we generated *Il17a*$^{-/-}$, *Il17f*$^{-/-}$, and *Il17a*$^{-/-}$*Il17f*$^{-/-}$ mice (Figure S1, available online). These mice were born healthy at the expected Mendelian ratio, were fertile, and showed no gross phenotypic abnormalities, including in their lymphoid cell populations (data not shown). Proliferative responses and interferon-γ (IFN-γ) production were normal in *Il17a*$^{-/-}$*Il17f*$^{-/-}$ mice, IL-17A production was normal in *Il17f*$^{-/-}$ mice, and neither IL-17A nor IL-17F was required for TGF-β plus IL-6-induced Th17 cell differentiation (Figure S2).

IL-17A plays a crucial role in the spontaneous development of arthritis in IL-1 receptor antagonist-deficient (*Il1rn*$^{-/-}$) mice (Nakae et al., 2003b). There were more IL-17F-producing cells, which also produced IL-17A, among the arthritic *Il1rn*$^{-/-}$ lymph node (LN) cells than among the wild-type LN cells, which was also true of the IFN-γ-producing cells (Horai et al., 2004) (Figure 1A). The IL-17A$^+$IL-17F$^+$ cell number and IL-17A and IL-17F mRNA expression were also augmented in LN cells from arthritic *Il1rn*$^{-/-}$ mice (Figures 1B and 1C). The development of arthritis was considerably, but only partially, suppressed in *Il17f*$^{-/-}$ *Il1rn*$^{-/-}$ mice compared with littermate *Il17f*$^{+/+}$*Il1m*$^{-/-}$ and *Il17f*$^{+/-}$*Il1rn*$^{-/-}$ controls during the 30 week observation period (Figure 1D). Compared with *Il17f*$^{-/-}$*Il1rn*$^{-/-}$ mice, arthritis development was markedly suppressed in *Il17a*$^{-/-}$*Il17f*$^{-/-}$*Il1m*$^{-/-}$ mice (Figure 1D). The IL-17A$^+$ T cell populations in LNs from *Il17a*$^{+/+}$*Il17f*$^{+/+}$*Il1m*$^{-/-}$ and *Il17f*$^{-/-}$*Il1rn*$^{-/-}$ mice were similar (Figure 1E).

Likewise, EAE, CIA, DTH, 2,4,6-trinitrochlorobenzene (TNCB)-induced CHS, and neutrophilic airway inflammation induced by OVA in DO11.10 mice, in which IL-17A plays an important role (Komiyama et al., 2006; Nakae et al., 2002, 2003a, 2007), also developed normally in the *Il17f*$^{-/-}$ mice (Figures S3–S7, and Table S1). These results indicate that IL-17A plays a major role in T cell-dependent autoimmune and allergic responses, but IL-17F only marginally contributes to these responses, if at all.

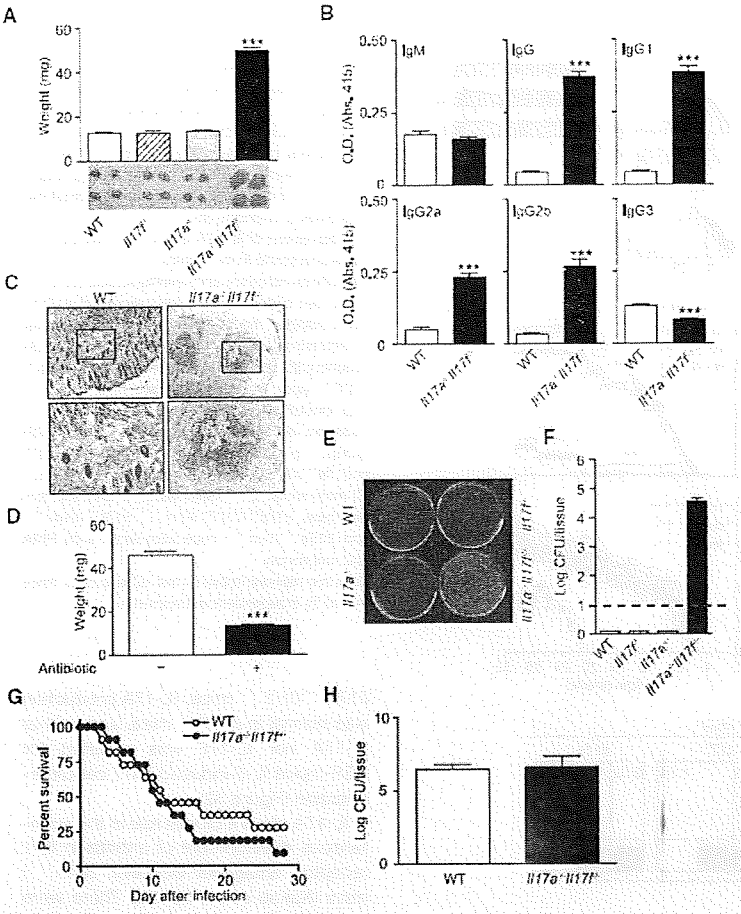

Figure 2. Increased Susceptibility of *Il17a*$^{-/-}$*Il17f*$^{-/-}$ Mice to Opportunistic *S. aureus* Infection

(A) Weight and gross morphology of submandibular LNs from BALB/cA mice at 12–16 weeks of age (n = 3–8/group).

(B) Immunoglobulin titers in sera from mice at 8–10 weeks of age (n = 6–8/group). Similar results were also observed on a C57BL/6J background.

(C) Histopathology of *Il17a*$^{-/-}$*Il17f*$^{-/-}$ mucocutaneous tissues around the nose and mouth (H&E, top, 40×; bottom, 120×). Data are representative of four mice for each group.

(D) Weight of submandibular LNs from *Il17a*$^{-/-}$*Il17f*$^{-/-}$ mice on a BALB/cA background with or without oral antibiotic treatment between 4 and 8 weeks of age (n = 10/group).

(E) Representative plates showing bacterial colonies recovered from mucocutaneous tissues of BALB/cA mice at 12–16 weeks of age.

(F) CFU of *S. aureus* in homogenates from mucocutaneous tissues in mice at 12–16 weeks of age. Data are pooled from three independent experiments.

(G) Survival rate in mice after intravenous (i.v.) injection of 1 × 10^7 CFU of *S. aureus* (n = 11/group). Data are representative of two independent experiments.

(H) *S. aureus* CFUs in kidney homogenates collected 3 days after i.v. injection of 1 × 10^7 CFU of *S. aureus* (n = 4/group). Data are representative of two independent experiments.

* $p < 0.05$, ** $p < 0.05$, and *** $p < 0.05$ versus wild-type. Data represent means ± SEM in (B), (D), (F), and (H).

Il17a$^{-/-}$*Il17f*$^{-/-}$ Mice Show Increased Susceptibility to Opportunistic Infection by *S. aureus*

We found that the submandibular LNs of *Il17a*$^{-/-}$*Il17f*$^{-/-}$ mice, but not of wild-type, *Il17f*$^{-/-}$, or *Il17a*$^{-/-}$ mice, became enlarged as the mice aged; this effect was observed in various genetic backgrounds, including the C57BL/6J, BALB/cA, and 129/Ola × C57BL/6J strains (Figure 2A, and data not shown). At 8–10 weeks of age, IgM titers were similar between *Il17a*$^{-/-}$*Il17f*$^{-/-}$ and wild-type mice. Whereas total IgG, IgG1, IgG2a, and IgG2b titers were increased 2–4 fold in the *Il17a*$^{-/-}$*Il17f*$^{-/-}$ mice compared with wild-type mice, IgG3 titers in the *Il17a*$^{-/-}$*Il17f*$^{-/-}$ mice were reduced (Figure 2B). Interestingly, the *Il17a*$^{-/-}$*Il17f*$^{-/-}$ mice developed mucocutaneous abscesses around the nose and mouth (Figure 2C). Histological analyses revealed fibrin-encased abscesses and marked leukocyte infiltration specifically in the mucocutaneous tissues of the *Il17a*$^{-/-}$*Il17f*$^{-/-}$ mice.

The LN enlargement, subcutaneous abscess formation, and increased Ab production suggested that the *Il17a*$^{-/-}$*Il17f*$^{-/-}$ mice may have been responding to an infection. In support of this idea, antibiotic treatment suppressed the enlargement of submandibular LNs in *Il17a*$^{-/-}$*Il17f*$^{-/-}$ mice (Figure 2D). Then, we tried to recover infected microorganisms from the mucocutaneous tissues around the nose and mouth of the *Il17a*$^{-/-}$*Il17f*$^{-/-}$ mice; the opportunistic bacterium *Staphylococcus aureus* was recovered from the affected tissues of these mice. When mucocutaneous tissue homogenates from these mice were cultured, more bacteria was observed in *Il17a*$^{-/-}$*Il17f*$^{-/-}$ mouse homogenate compared with samples from wild-type, *Il17f*$^{-/-}$, and *Il17a*$^{-/-}$ mice (Figures 2E and 2F), suggesting that both IL-17A and IL-17F are critically important to protect the mice against mucocutaneous *S. aureus* infections. To investigate whether IL-17A and IL-17F play a role in systemic *S. aureus* infection, we challenged mice with *S. aureus* by intravenous injection. However, no difference was observed in the survival and the number of bacteria recovered from the kidney 72 hr later between wild-type and *Il17a*$^{-/-}$*Il17f*$^{-/-}$ mice (Figures 2G and 2H). These results suggest that both IL-17A and IL-17F play critical roles in protecting against local, but not systemic, infection against *S. aureus*.

Both IL-17F and IL-17A Are Required for Host Defense against *C. rodentium* Infections

Because the *Il17a*$^{-/-}$*Il17f*$^{-/-}$ mice were susceptible to opportunistic infections by *S. aureus*, we examined the susceptibilities of *Il17f*$^{-/-}$, *Il17a*$^{-/-}$, and *Il17a*$^{-/-}$*Il17f*$^{-/-}$ mice to experimental

C. rodentium infection. After oral infection with *C. rodentium*, the number of bacteria in the colons of wild-type 129/Ola × C57BL/6J mice increased until 14 days after infection, and decreased thereafter (Figure 3A). A substantially greater number of bacteria was detected in the colons of *Il17f*$^{-/-}$, *Il17a*$^{-/-}$, and *Il17a*$^{-/-}$*Il17f*$^{-/-}$ mice compared with wild-type mice at each time point after infection, although the bacterial burden in the mutant mice declined by day 21 and all of the genotypes returned to the wild-type level by day 28 after infection. Notably, bacterial numbers in the colon were similar among *Il17f*$^{-/-}$, *Il17a*$^{-/-}$, and *Il17a*$^{-/-}$*Il17f*$^{-/-}$ mice. Marked expansion of the bacterial population was also observed in the distal colon of *Il17f*$^{-/-}$, *Il17a*$^{-/-}$, and *Il17a*$^{-/-}$*Il17f*$^{-/-}$ mice compared with that of wild-type mice 14 days after infection (Figure 3B). Furthermore, whereas remarkable hypertrophy of the colon and spleen was observed in *Il17f*$^{-/-}$ and *Il17a*$^{-/-}$*Il17f*$^{-/-}$ mice, only mild hypertrophy was detected in *Il17a*$^{-/-}$ mice (Figures 3C and 3D). Consistent with these observations, more severe inflammatory changes were observed in the colons of *Il17f*$^{-/-}$ and *Il17a*$^{-/-}$ *Il17f*$^{-/-}$ mice compared to *Il17a*$^{-/-}$ mice 14 days after infection, suggesting that IL-17F plays a larger role than IL-17A in the immune response against this bacterium (Figures 3E and 3F). These observations clearly show that both IL-17A and IL-17F play important roles to protect hosts against *C. rodentium* infections.

IL-17F and IL-17A Are Required for the Expression of β-Defensin in the Colon

Then, we analyzed the antibacterial mechanisms induced by IL-17A and IL-17F. The serum amounts of *C. rodentium*-specific IgG, which is important for bacterial clearance (Mundy et al., 2005), were increased in all of the mutant mice (Figure S8), suggesting that the humoral immune response against *C. rodentium* was not responsible for delayed bacterial clearance in the *Il17f*$^{-/-}$, *Il17a*$^{-/-}$, and *Il17a*$^{-/-}$*Il17f*$^{-/-}$ mice.

Both IL-17A and IL-17F regulate innate immunity by inducing neutrophil recruitment and antimicrobial peptide production (Ouyang et al., 2008). Compared to wild-type mice, however, mRNA expression of neutrophil chemoattractants, such as CXCL1 and CXCL2, and proinflammatory mediators, such as IFN-γ, IL-1β, IL-6, TNF, and iNOS, were similarly increased in the colons of *Il17f*$^{-/-}$, *Il17a*$^{-/-}$, and *Il17a*$^{-/-}$*Il17f*$^{-/-}$ mice 14 days after *C. rodentium* infection (Figure 4A). However, the expression of antimicrobial peptides, such as β-defensin 1, 3, and 4 (but not β-defensin 2, lipocalin 2, S100A8, S100A9, Reg3β, and Reg3γ), was markedly impaired in the colons of *Il17f*$^{-/-}$, *Il17a*$^{-/-}$, and *Il17a*$^{-/-}$*Il17f*$^{-/-}$ mice on day 14 after *C. rodentium* infection (Figure 4B). These results suggest that both IL-17F and IL-17A are critical to induce the expression of β-defensins, which are important for the host defense against *C. rodentium*.

IL-17F and IL-17A Are Produced by Different Cells in the Colon

IL-17A mRNA is more highly expressed in the small intestine than in the colon (Ivanov et al., 2006). In contrast, IL-17F mRNA expression in the colon was higher than that in the small intestine (Figure 5A). During *C. rodentium* infection, the expression of both IL-17A and IL-17F mRNA was induced in the colon of wild-type mice, although a larger increase was observed for IL-17A mRNA expression (day 14: IL-17A, 29-fold; IL-17F, 14-fold) (Figure 5B). Under these conditions, IL-17A mRNA expression was not influenced by IL-17F deficiency and vice versa. Although only a few IL-17A- and IL-17F-producing cells were found among the colonic lymphocytes of uninfected wild-type mice (Figure 5C), the population of IL-17F-producing cells, which also produced IL-17A, increased in infected wild-type mice (Figure 5D). In contrast to the coordinate production of IL-17A and IL-17F by LN cells after the development of DTH, EAE, or arthritis (Figure 1A and Figure S5), however, the percentage of IL-17A^{+}IL-17F^{-} cells in the colonic lymphocytes was much larger than that of IL-17A^{-}IL-17F^{+} cells (Figure 5D). Both IL-17A^{+} and IL-17F^{+} cells were not observed in the *Il17a*$^{-/-}$*Il17f*$^{-/-}$ colonic lymphocyte population, whereas the number of IFN-γ^{+} cells markedly increased during *C. rodentium* infection (Figure 5D).

Because the induction kinetics was different for the two molecules and IL-17F producer cells were scarcely found in colonic lymphocytes, IL-17A and IL-17F may be produced by different cells in the colon. The mRNA expression of these molecules was examined in the colons of recombination activating gene-2-deficient (*Rag2*$^{-/-}$) mice, in which both T and B cells are absent. The expression of IL-17A mRNA in the mesenteric LNs (MLNs) was markedly higher than that in colons on day 7 after *C. rodentium* infection in wild-type mice (Figure 5E). The amount of IL-17A mRNA, however, was markedly decreased (approximately 20% of wild-type) in *Rag2*$^{-/-}$ mice (Figures 5E and 5F), suggesting that Th17 cells may be the major producer of IL-17A in the MLN. In contrast, the amount of IL-17F expression was only decreased by approximately 50% in the MLNs of these mice (Figures 5E and 5F). IL-17A mRNA expression was also markedly decreased in the colons of *Rag2*$^{-/-}$ mice, whereas the IL-17F mRNA expression was similar between wild-type and *Rag2*$^{-/-}$ mice (Figures 5E and 5F). In addition, IL-17F, but not IL-17A, production in the whole-colon-culture supernatants from *Rag2*$^{-/-}$ mice was increased by the treatment with IL-23, whereas both IL-17A and IL-17F production were induced in those from wild-type mice, indicating that IL-17F is also produced by non-T and non-B cells (Figure 5G). We next examined which cells produce IL-17F in response to IL-23. Interestingly, IL-23 stimulation led to enhanced IL-17F production in splenocytes or MLNs from *Rag2*$^{-/-}$ or C.B-17 SCID mice compared to those from wild-type mice, whereas only a small amount of IL-17A was produced in these cells (Figures 5H and 5I, and Figure S9). Among innate immune cells, CD11c^{-} Gr1^{-} B220^{-} F4/F80^{-} Gr1^{-} cells were likely to mainly produce IL-17F upon IL-23 stimulation (Figure S9).

Because IL-17F is expressed in lung epithelial cells (ECs) (Suzuki et al., 2007), we also examined whether IL-17F was expressed in colonic ECs. IL-17F mRNA, but not IL-17A mRNA, was detected in CD45^{-} FACS-sorted colonic ECs from infected wild-type mice; this contrasted to CD45^{+} intraepithelial immune cells and ConA-stimulated splenocytes, in which both IL-17A and IL-17F were detected (Figure 5J). Moreover, IL-17F, but not IL-17A, mRNA was expressed in mouse colonic EC lines (Figure 5K). These results indicate that, in addition to infiltrating lymphocytes, IL-17F is produced by non-T, non-B innate immune cells and colonic ECs in response to infection with *C. rodentium*.

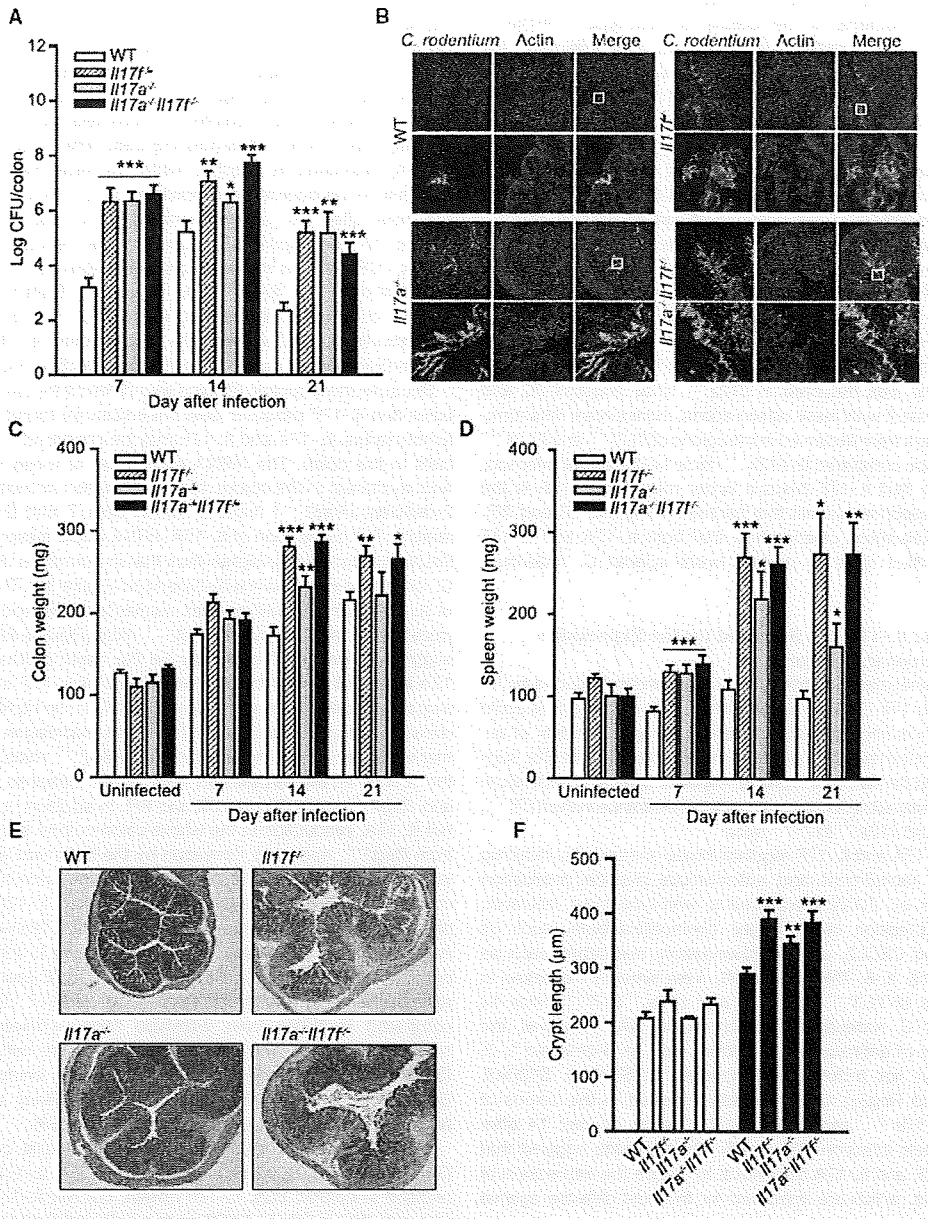

Figure 3. IL-17F and IL-17A Are Required for the Protection against *C. rodentium* Infection

Wild-type, *Il17f*$^{-/-}$, *Il17a*$^{-/-}$, and *Il17a*$^{-/-}$*Il17f*$^{-/-}$ mice were orally infected with 2 × 10^{8} CFU of *C. rodentium*, and the colons and spleens were harvested at the indicated time points after infection.

(A) *C. rodentium* CFUs in colon homogenates (n = 10–16/group). Data show pooled results from two or three independent experiments.

(B) Visualization of *C. rodentium* in the distal colon 14 days after oral infection (top, 40×; bottom, 120×). Data are representative of four to six mice for each group.

(C and D) Colon weight (C) and spleen weight (D) after oral infection as shown in (A). Data show pooled results from two or three independent experiments (n = 10–16/group).

(E and F) Histopathology (E) and crypt length (F) in the distal colon 14 days after oral infection (H&E, 40×). Data are pooled from two or three independent experiments (uninfected, n = 3/group; day 14, n = 20–23/group). In (F), white bars represent uninfected mice, and black bars represent day 14 mice.

* $p < 0.05$, ** $p < 0.01$, and *** $p < 0.001$ versus wild-type mice. Data represent means ± SEM in (A) and (C)–(F).

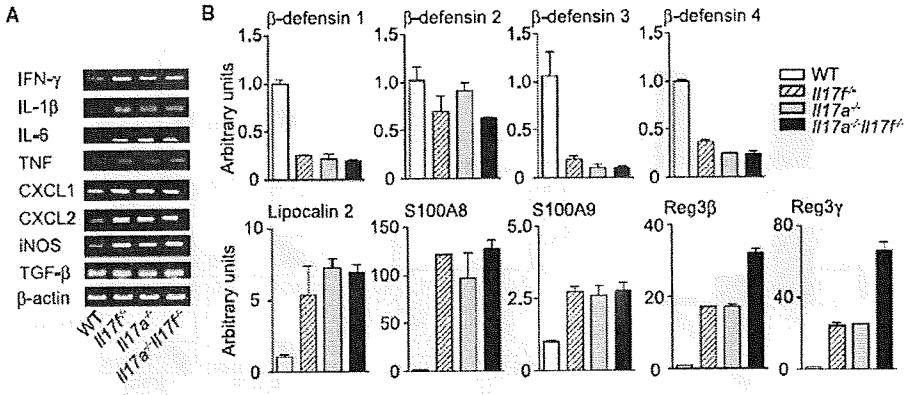

Figure 4. IL-17F and IL-17A Are Required for the Induction of β-Defensin Expression during *C. rodentium* Infection
(A) The expression of inflammatory mediators in the colon 14 days after infection with *C. rodentium* was determined with semiquantitative RT-PCR.
(B) The expression of antimicrobial peptide in the colon 14 days after infection with *C. rodentium* was determined with real-time RT-PCR. Data represent the means ± SEM. The RNA sample was pooled from six to eight mice for each group.
All data are representative of three independent experiments.

IL-17RC Is Highly Expressed in Colonic Epithelial Cells

Two receptor molecules, IL-17RA and IL-17RC, reportedly bind IL-17A and IL-17F (Toy et al., 2006; Zheng et al., 2008). Because the binding affinities of IL-17A and IL-17F for these receptors are different (Hymowitz et al., 2001; Kuestner et al., 2007; Wright et al., 2008), we examined the tissue distribution of these molecules. As reported previously (Kuestner et al., 2007), IL-17RA mRNA was highly expressed in such lymphoid tissues as the thymus, spleen, and LNs (Figure 6A). On the other hand, IL-17RC mRNA was expressed at high amounts in such nonhematopoietic tissues as the colon, small intestine, and lung (Figure 6A). Consistent with these observations, T and macrophage cell lines expressed higher amounts of IL-17RA mRNA than a colonic EC line, whereas the colonic EC line expressed higher amounts of IL-17RC mRNA than the T cell line (Figure 6B). We also found that IL-17RA or Act1 mRNA was constitutively expressed in Thy1.2$^+$ cells, B220$^+$ cells, CD11c$^+$ cells, CD11b$^+$ cells, peritoneal macrophages, and colonic epithelial cells (CMT93), whereas IL-17RC mRNA was detected only peritoneal macrophages and colonic ECs (Figure 6C). Thus, the tissues distributions of these receptors are strikingly different, and colonic ECs preferentially express IL-17RC.

We next examined whether IL-17F can transduce signals to T cells, peritoneal macrophages, or colonic epithelial cells. We found that IL-17A could induce IL-6 by peritoneal macrophages, CCL2 by CD4$^+$ T cells, or lipocalin 2 and β-defensin 3 by colonic epithelial cells (CMT93) in a dose-dependent manner (Figures 6D–6F), and 50 ng/ml of IL-17A was sufficient to induce several cytokines and chemokines by these cells (Figures 6D–6I and Figure S10). The cytokine-inducing activity of IL-17A was not the effect of contaminated LPS, because we found that IL-6 production was observed in IL-17A-treated peritoneal macrophages from both C3H/HeN (LPS-sensitive) and C3H/HeJ (LPS-insensitive) mice (Figure 6D). However, whereas IL-6, CCL3, and G-CSF production were induced in peritoneal macrophages by the treatment with IL-17F (50 ng/ml), this cytokine could not increase other inflammatory mediators, which was induced by IL-17A (Figures 6D and 6H and Figure S10). In contrast, similar to IL-17A, treatment of IL-17F in colonic epithelial cells induced most of inflammatory mediators examined, although the activity of IL-17F was slightly lower compared to that of IL-17A (Figures 6F and 6G and Figure S10). IL-17A, but not IL-17F, also induced several cytokine and chemokine production in CD4$^+$ T cells. We could not observe any synergy between IL-17A and IL-17F (Figures 6F, 6G, and 6I and Figure S10). Thus, these observations suggest that IL-17A and IL-17F can differentially induce the expression of cytokines and antimicrobial peptides in a cell-type-specific manner.

DISCUSSION

In this report, we have demonstrated that IL-17A is critical for the development of DTH, CHS, EAE, CIA, and arthritis in *Il1m*$^{-/-}$ mice, whereas IL-17F is not only dispensable for the induction of these responses, but also does not have any substantial additive, synergistic, or compensatory effects to those of IL-17A in these disorders. These observations suggest that IL-17F has only low activity compared to IL-17A in these immune responses, although IL-17A and IL-17F are produced simultaneously by Th17 cells and bind the same receptors. In this regard, we found that cytokine-inducing activity of IL-17F from macrophages or T cells was much lower than IL-17A. Because IL-17A enhances immune responses by activating T cell priming (Nakae et al., 2002, 2003b), and induces inflammation by inducing cytokines from various types of cells including macrophages (Da Silva et al., 2008; Jovanovic et al., 1998) and dendritic cells (Antonysamy et al., 1999; Coury et al., 2008), this low cytokine-inducing activity of IL-17F on immune cells may be responsible for the inefficiency of this cytokine in allergic and autoimmune responses.

We showed that *Il17a*$^{-/-}$*Il17f*$^{-/-}$ mice were sensitive to opportunistic infection with *S. aureus*, indicating that IL-17A and IL-17F are important for host defense against this bacterium. Consistent with this observation, increased susceptibility to *S. aureus* was

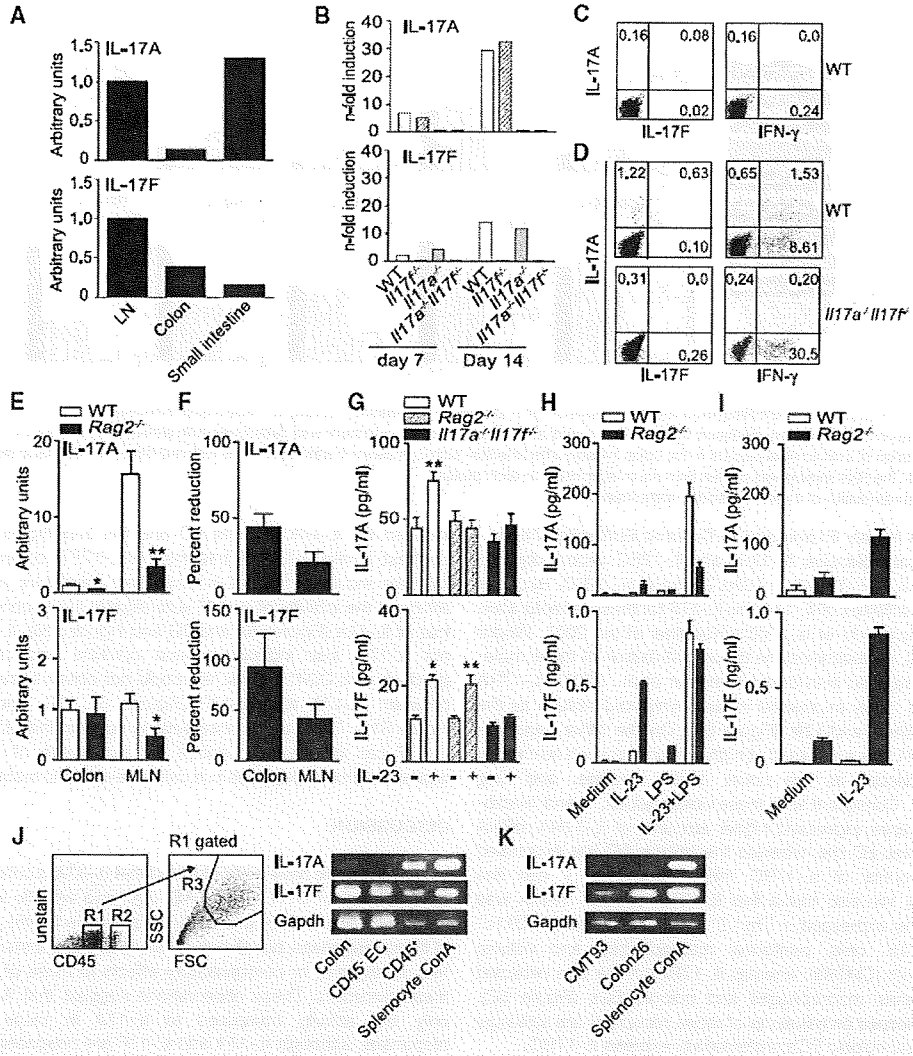

Figure 5. IL-17F and IL-17A Are Produced by Different Cells

(A) Colon, small intestine, and peripheral LNs from wild-type mice were analyzed for IL-17A and IL-17F mRNA expression with real-time RT-PCR. Expression in LN cells was defined as 1.

(B) The expression of IL-17A and IL-17F in the colons of mice 7 and 14 days after infection with *C. rodentium* was determined with real-time RT-PCR. The RNA sample was a pool of samples from four to six mice for each group. The expression in uninfected wild-type mice was defined as 1.

(C and D) Profiles of intracellular IL-17F, IL-17A, and IFN-γ expression in colonic PMA- and ionomycin-stimulated lymphocytes from uninfected mice (C) or mice 14 days after infection with *C. rodentium* (D).

(E and F) The colons and MLNs of C57BL/6J wild-type and *Rag2*$^{-/-}$ mice 7 days after infection with *C. rodentium* were analyzed for IL-17A and IL-17F mRNA expression with real-time RT-PCRs (E) (n = 5–6/group). The expression in wild-type colon was defined as 1. The expression of these cytokines in the colon and MLNs of *Rag2*$^{-/-}$ mice was determined as a percentage of the expression in wild-type mice (F).

(G) Whole colons of uninfected wild-type, *Rag2*$^{-/-}$, and *Il17a*$^{-/-}$*Il17f*$^{-/-}$ mice were cultured for 24 hr in the presence or absence of 20 ng/ml IL-23. The concentrations of IL-17A or IL-17F in supernatant were determined by ELISAs and were normalized to total protein content for each sample (n = 5–8/group). Similar results were also observed in C.B-17 SCID mice.

(H and I) Splenocytes (5 × 10^5 cells) (H) or MLNs (1.5 × 10^5 cells) (I) of wild-type and *Rag2*$^{-/-}$ mice were cultured in 24- or 48-well plates, respectively, in the presence or absence of 5 μg/ml LPS and 20 ng/ml IL-23 for 72 hr, and IL-17A and IL-17F amounts in culture supernatants were determined with ELISA.

(J) Colonic epithelial (CD45$^-$ and high FSC and SSC; gates R1 and R3) cells and intraepithelial immune cells (CD45$^+$; gate R2) were isolated from the colons of uninfected wild-type mice with flow cytometry, and the expression of IL-17F and IL-17A was examined with RT-PCR.

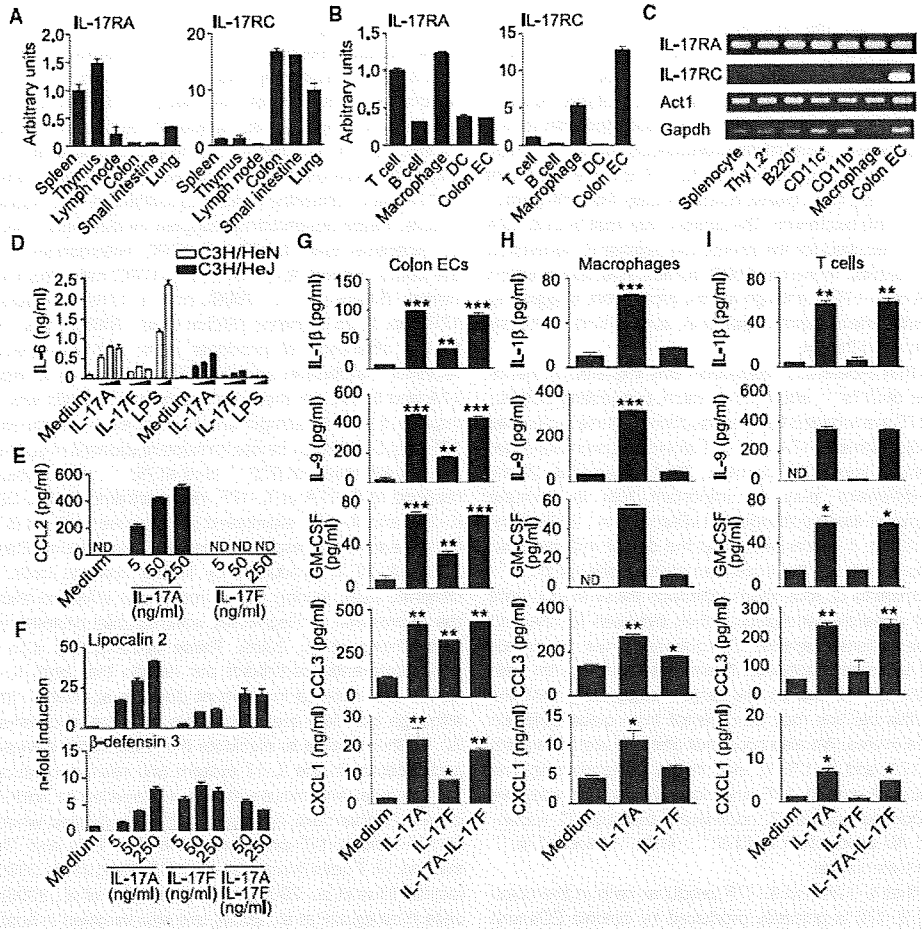

Figure 6. IL-17RA and IL-17RC Show Different Tissue Distributions

(A and B) The expression of IL-17RA and IL-17RC in tissues from 129/Ola × C57BL/6J wild-type mice (A), and different cell lines (B) were determined with real-time RT-PCR.

(C) The expression of IL-17RA, IL-17RC, and Act1 in different cell populations obtained by MACS sorting was determined with RT-PCR.

(D) Peritoneal macrophages were stimulated for 24 hr with 5–250 ng/ml IL-17A or IL-17F, or 10–100 ng/ml LPS, and IL-6 amounts in the culture supernatants were determined with ELISAs.

(E) $CD4^+$ T cells from C57BL/6J mice obtained by MACS sorting were stimulated for 48 hr with 5–250 ng/ml IL-17A or IL-17F, and CCL2 in the culture supernatants was determined with Bio-Plex suspension array system (Bio-Rad).

(F) The expression of lipocalin 2 and β-defensin 3 in colonic epithelial cell line (CMT93) stimulated for 6 hr with 5–250 ng/ml IL-17A or IL-17F individually, or with combination of 50–250 ng/ml IL-17A and IL-17F, was determined with real-time RT-PCR.

(G–I) Colonic epithelial cell line (CMT93) (G), peritoneal macrophages from C3H/HeJ mice (H), or $CD4^+$ T cells from C57BL/6J mice (I) were stimulated for 24 hr (G and H) or 48 hr (I) with 50 ng/ml IL-17A or IL-17F individually, or with a combination of 50 ng/ml IL-17A and IL-17F. IL-1β, IL-9, GM-CSF, CCL3, or CXCL1 in the culture supernatants were determined with the Bio-Plex suspension array system (Bio-Rad). ND denotes not detected. * $p < 0.05$, ** $p < 0.01$, and *** $p < 0.001$ versus medium alone.

All data represent means ± SEM and are representative of three independent experiments.

reported in *Il17ra*$^{-/-}$ mice (Schwarzenberger and Kolls, 2002) and subjects with mutations in STAT3, in whom Th17 cell differentiation and function is impaired (Milner et al., 2008). Because *Il17f*$^{-/-}$ and *Il17a*$^{-/-}$ mice showed normal sensitivities to *S. aureus*, IL-17A and IL-17F complement each other in this setting. Furthermore, we showed that IL-17A and IL-17F are

(K) The expression of IL-17A and IL-17F in mouse colonic epithelial cell line (CMT93 or Colon 26) was examined with RT-PCR.

Data are representative of two (A, B, and K) or three (C–J) independent experiments. Data represent means ± SEM in (E)–(I).